EXTENDIBLE-RETRACTABLE ELECTRIC FIELD MEASUREMENT ANTENNA FOR IMP J

Final Report

Contract NAS 5-23063

August 24, 1973

Prepared For:

National Aeronautics and Space Administration
Goddard Space Flight Center
Greenbelt, Maryland

Prepared By:

EMR Aerospace Sciences
EMR Division
Weston Instruments, Inc.
College Park, Maryland
301-864-6340

TECHNICAL REPORT STANDARD TITLE PAGE

1. Report No.	2. Government Accession No.	3. Recipient's Catalog No.
6341-2060		

4. Title and Subtitle	5. Report Date
Extendible-Retractable Electric Field Measurement Antenna for IMP J	August, 1973
	6. Performing Organization Code
7. Author(s)	8. Performing Organization Report No.
Wayne Larrick	
9. Performing Organization Name and Address	10. Work Unit No.
EMR Aerospace Sciences 5012 College Avenue College Park, Maryland 20740	11. Contract or Grant No. NAS 5-23063
	13. Type of Report and Period Covered Type III, Final Dec 1971-Aug 1973
12. Sponsoring Agency Name and Address	14. Sponsoring Agency Code
NASA, Goddard Space Flight Center Greenbelt, Maryland Wayne Sours, Technical Officer	

15. Supplementary Notes

16. Abstract

17. Key Words (Selected by Author(s))	18. Distribution Statement

19. Security Classif. (of this report)	20. Security Classif. (of this page)	21. No. of Pages	22. Price*
Unclassified	Unclassified		

*For sale by the Clearinghouse for Federal Scientific and Technical Information, Springfield, Virginia 22151.

TABLE OF CONTENTS

Applicable Specifications & References

1. NAS 5-23063 - EFM Antenna Contract

2. GSFC Specification S-721-P-2 "Extendible Retractable Electric Field Measurement Antenna for IMP-J" Revision B. July 20, 1971.

3. IMP-H & J, Mechanical Interface Document, September 1969.

4. IMP-H & J Specifications for Electrical Interfaces, October 1969.

List of Illustrations

PREFACE

EMR Aerospace Sciences has designed, fabricated and tested an antenna dispenser mechanism for the IMP J Spacecraft. Upon command the mechanism deploys or retracts a conductor for use as a receiving antenna for an Electric Field Measurement experiment.

Five identical units were fabricated and tested to the IMP H & J Environmental Test Specification. Of these, four are designated for flight on the IMP J Spacecraft and one as a prototype flight spare.

The testing program was successfully completed although certain design modifications were required as problems were uncovered by the testing; particularly Thermal Vacuum operation.

The antenna mechanism functions well under the expected environmental and loading conditions. The wear life and load capability of the dry molybdenum disulphide lubricant originally used on the heavily loaded worm and gear pair were disappointing and a substitute material developed by the GSFC materials sections was applied.

The lubricant finally applied performed well; although other problems were generated.

The use of dry lubricants for unsealed space application is mandatory. More effort should be made to solve this worm gear lubrication problem for any future units. The insulation chosen (FEP teflon) for the antenna conductor is very easily damaged by handling. A tougher coating is extremely desirable. It is recommended that KAPTON wire be considered for use on future units and that a short program of bench and thermal vacuum operation be performed with KAPTON wire and the prototype mechanism when it becomes available from its present flight space function.

1.0 INTRODUCTION

The system EMR has designed provides a unique method for precisely controlling the deployment and retraction rate of the antennas by using a hysteresis synchronous motor whose angular velocity is a direct function of the driving frequency. To provide a precise drive source, EMR has designed a unique circuit which utilizes a stable square wave to generate a waveform which drives the motor at nearly sine wave efficiency. A significant item in EMR's design is the use of a storage reel with a helical groove and associated traveling guide for antenna storage. This results in the antenna wire always being stored in the same configuration, preventing creep wire distortion and wire slump.

The following discussions describe in detail a system offering these significant advantages:

Unique and highly efficient antenna drive
Precise control and measurement of antenna position
No brake required to withstand centrifugal force
Accurate tracking of antenna deployment rates

Typical characteristics for the system.

1)	Weight	7.5 lbs
2)	Antenna length (deployed) 195 ft, stainless steel stranded wire (FEP teflon insulation).	
3)	Deployment or retraction rate	0.11 FPS
4)	Power (extend mode)	29 watts
5)	(retract mode)	22 watts
	Capacitance antenna to ground	
6)	Fully extended	$\approx$ 30 pf
7)	Fully retracted	$\approx$ 60 pf

2.0 SYSTEM DESCRIPTION

The IMP J EFM antenna system consists of four mechanisms arranged symmetrically about the spacecraft spin axis. Upon command the antenna conductor is deployed radially. The antenns function is receiving antennas for an electric field measurement experiment.

The deployment of the antennas increases the moment of inertia of the spacecraft and therefore reduces the spin rate. Final spin rate when the antennas are fully deployed is adjusted by spinning up the spacecraft with the attitude control system. If for any reason the spin rate should become too low and ACS propellant is not available, the mechanism may be retracted to increase the spin rate.

As the wire is deployed the centrifugal force creating tension in the wire is increased as a function of the increased radius and is decreased by the lowering of the spin rate. The spin rate is affected, not only by the changing moment of inertia, but by the planned spin-up with the ACS. Figures 2-A thru 2-D show plots of the spacecraft inertia and spin rate, as well as antenna tension, as the antennas are extended in a typical deployment scheme. These values were computed and plotted by GSFC, Code 732.

The antenna conductor is stored on a drum of slightly over 4 3/4 inches diameter which is arranged parallel to the long axis of the allowable volume as shown in Figure 2-1.

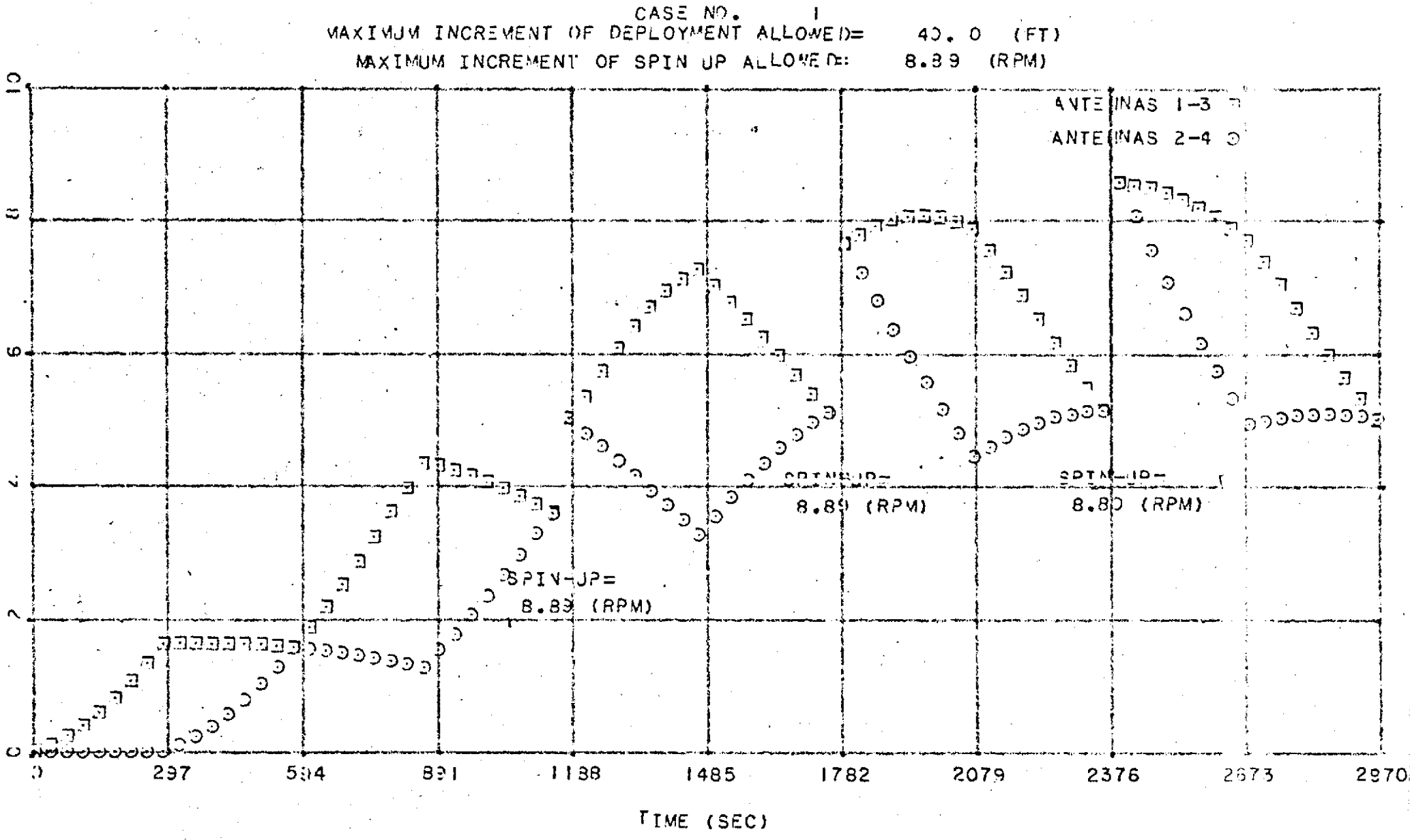
CASE NO. 1
MAXIMUM INCREMENT OF DEPLOYMENT ALLOWED= 40.0 (FT)
MAXIMUM INCREMENT OF SPIN UP ALLOWED: 8.89 (RPM)
ANTENAS 1-3
ANTENAS 2-4
SPIN-UP=
8.89 (RPM)
SPIN-UP=
8.89 (RPM)
SPIN-UP=
8.89 (RPM)
0
2
4
6
8
10
0
297
594
891
1188
1485
1782
2079
2376
2673
2970
TIME (SEC)

FIGURE 2-A

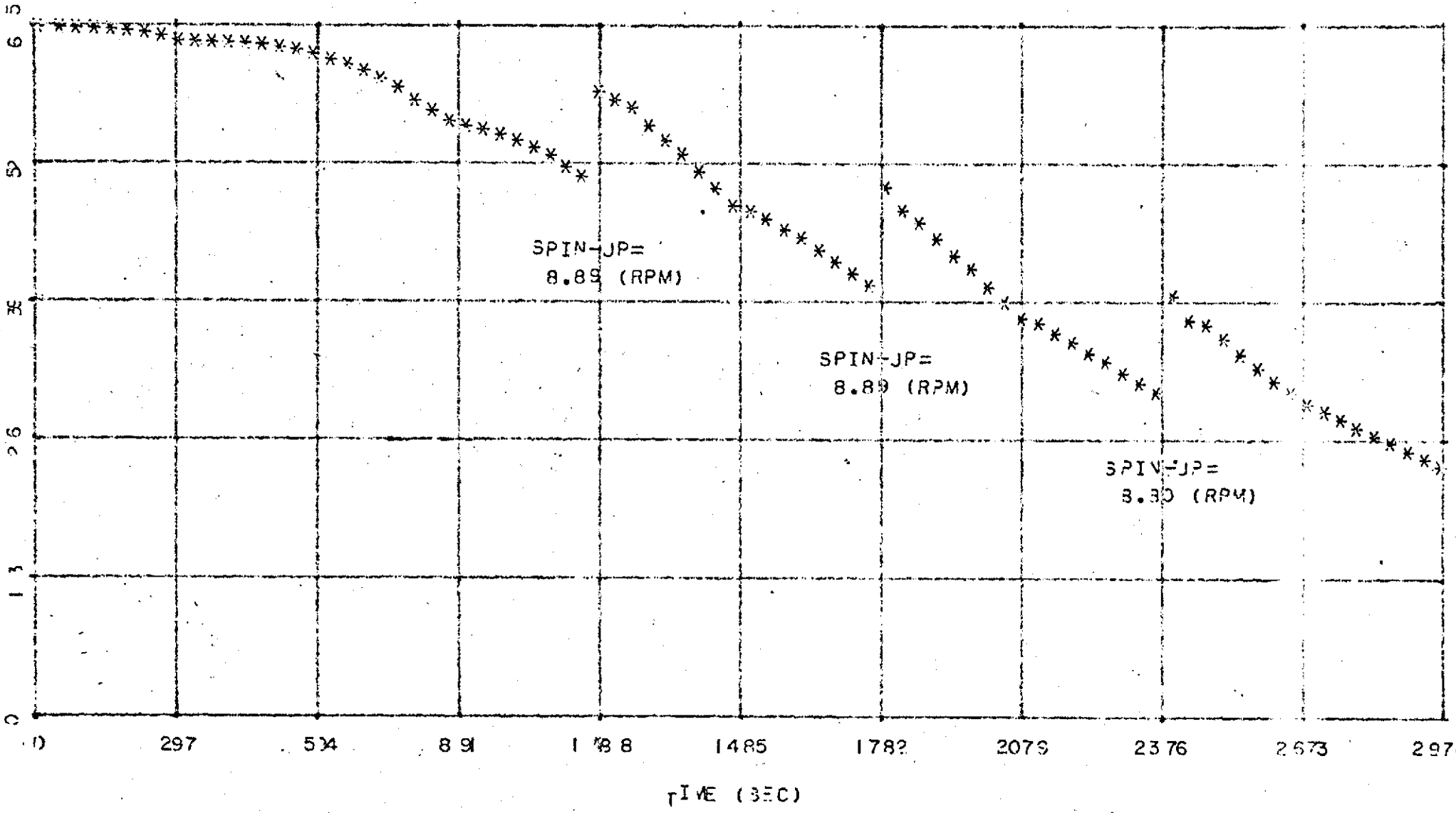
SPIN-JP=
8.89 (RPM)
SPIN-JP=
8.89 (RPM)
SPIN-JP=
8.89 (RPM)
0
297
534
891
1188
1485
1782
2079
2376
2673
TIME (SEC)

FIGURE 2-B

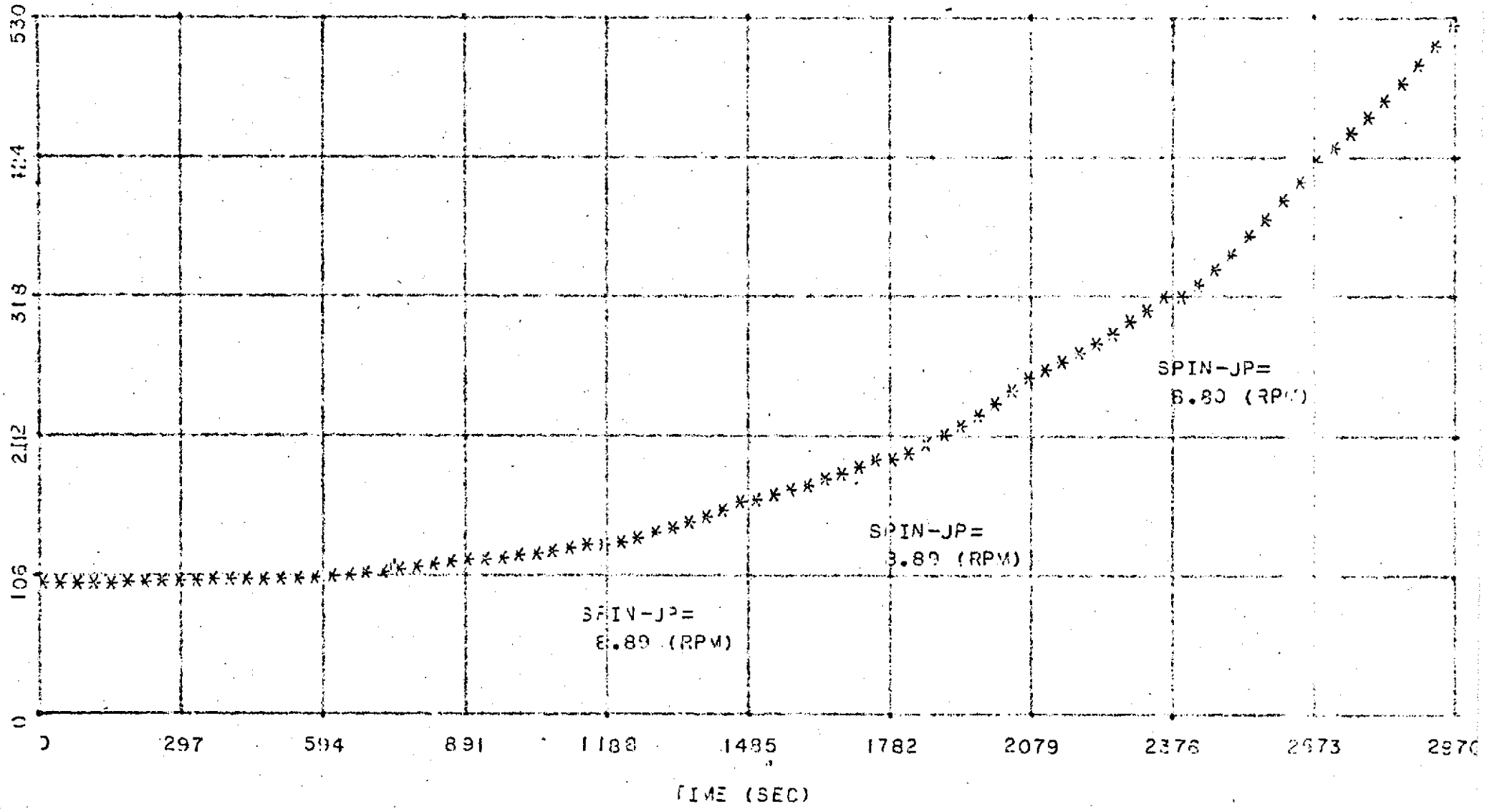
530
424
318
212
106
0
0
297
594
891
1188
1485
1782
2079
2376
2673
2970
TIME (SEC)
SPIN-JP=
8.89 (RPM)
SPIN-JP=
8.89 (RPM)
SPIN-JP=
8.89 (RPM)

FIGURE 2-C

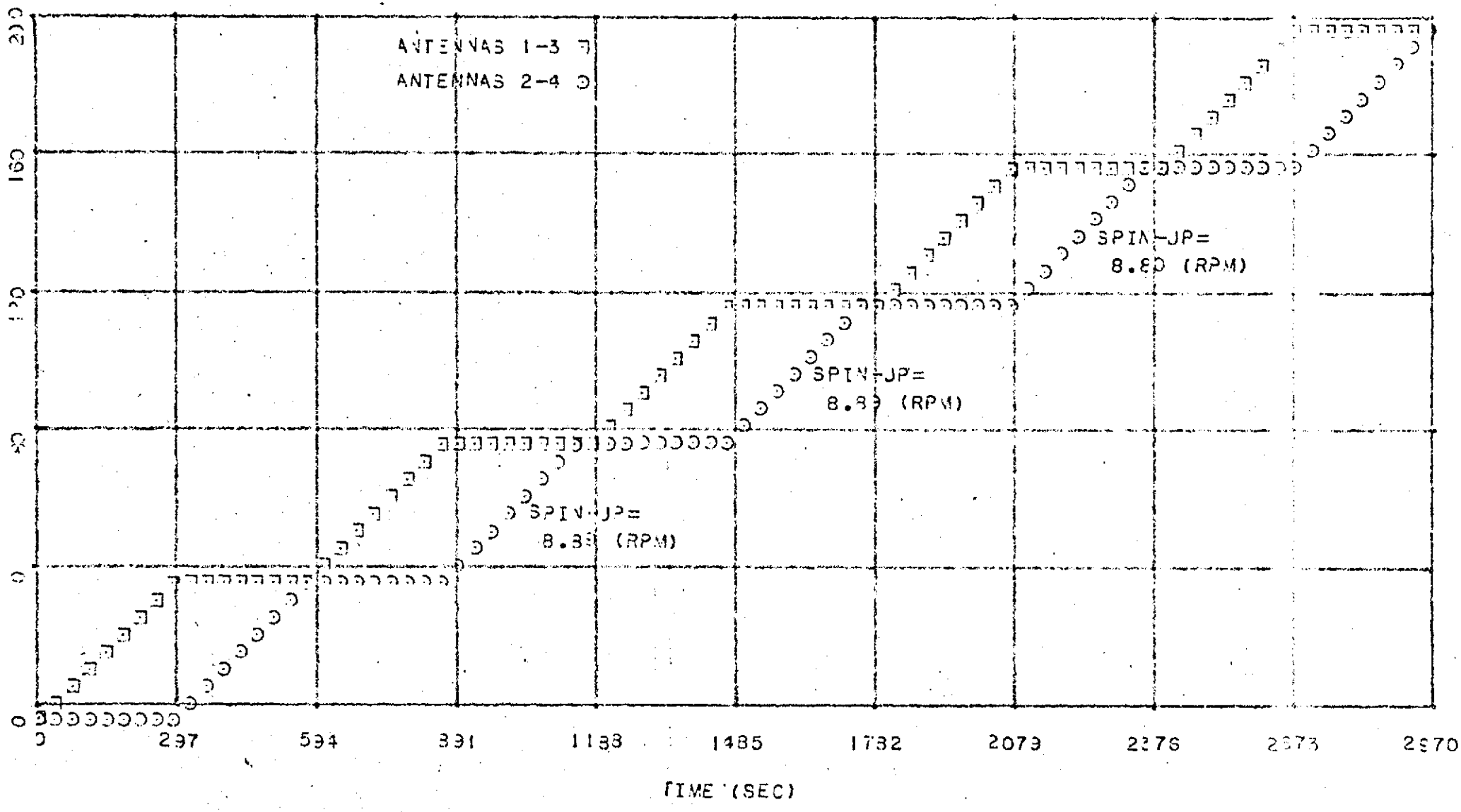
ANTENNAS 1-3
ANTENNAS 2-4
SPIN-UP=
8.8 (RPM)
SPIN-UP=
8.8 (RPM)
SPIN-UP=
8.8 (RPM)
0
297
594
891
1188
1485
1782
2079
2376
2673
2970
TIME (SEC)

FIGURE 2-D

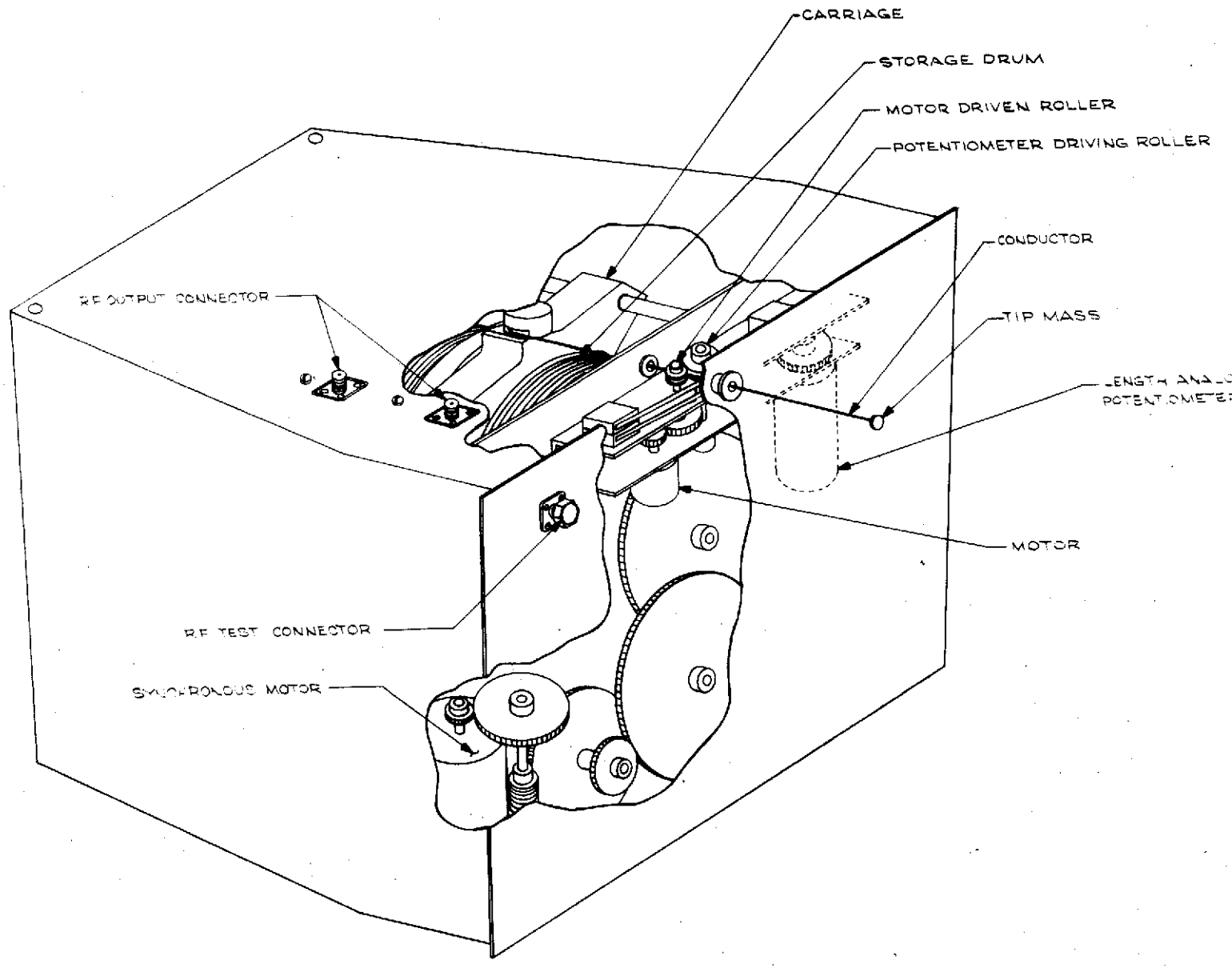

FIG. 2-1 ANTENNA DEPLOYMENT MECHANISM

A single layer wrap is used to avoid any looseness in packing with subsequent creep under an applied centrifugal loading. This avoids the requirement for special locking other than to prevent primary drum rotation. A shallow groove is generated on the surface of the cylinder. A traversing guide which arranges the conductor in the grooves makes one pass over the drum to fully store or deploy the conductor. As the guide reaches either extreme of its travel, it actuates a leaf switch which generates an event marker and, for safety, stops motor operation in that direction.

Figure 2-2 provides an electrical block diagram of the system. The storage reel is driven through a gear train by a hysteresis synchronous motor. This type of motor was selected by EMR in preference to a DC motor to obtain more precise speed control and minimize RF noise, and in preference to a stepper motor to increase efficiency and thus require less operating power. The waveform required to operate the motor is provided by a unique circuit which generates a modified square wave. Use of this waveform provides a drive which is substantially as efficient as a sine wave but requires no complicated and heavy filtering. Since the motor operates synchronously with the frequency of the drive waveform, precise speed control and thus matching of deployment rate is readily obtainable.

The GSFC specification requires the amount of antenna deployment to be measured by sensing the moving antenna wire. A number of electronic, mechanical and optical techniques were considered and the method chosen by EMR incorporates a separate torque motor driven roller and a second roller driving a potentiometer. The wire motion rotates the roller thus driving the potentiometer. The torque motor driven roller prevents slippage between the potentiometer roller and the wire and has the added advantage of adding a slight tension to the wire assuring that there will be no wire "slump" between the reel and the exit hole.

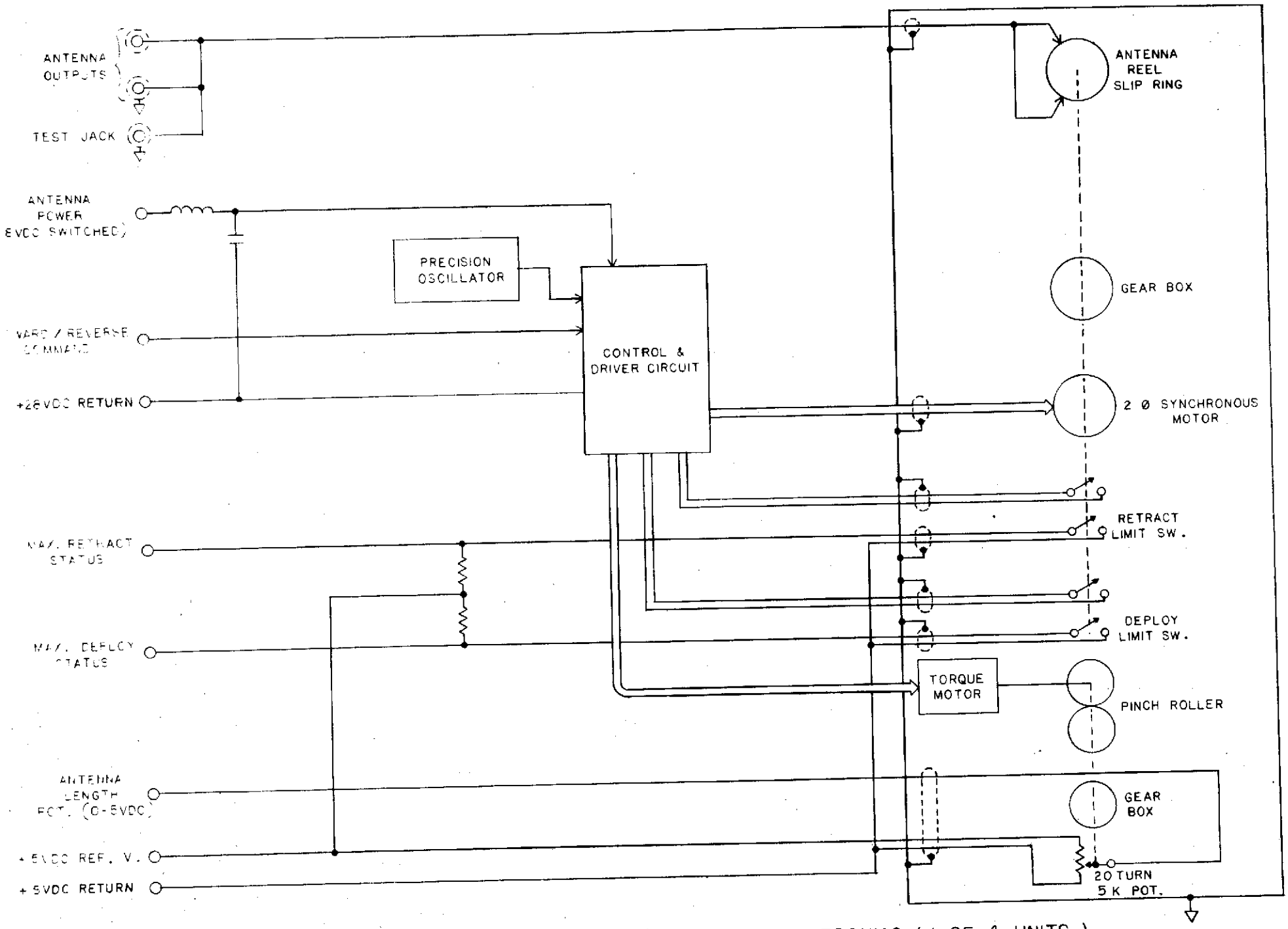

FIGURE 2-2 EFM ANTENNA DEPLOYMENT MECHANISM ELECTRONICS (1 OF 4 UNITS)

The antenna deployment system is mounted in a metal box divided into compartments. The discrete electronic components are assembled on two P. C. boards which are located in the electronics compartment. The reel compartment holds the antenna reel, motor, and multi-turn potentiometer. This compartment is sealed by a screw-down cover plate to make it RF tight. Electrical connections to the motor, potentiometer, brake and limit switches are shielded and filtered. The rear plate for this compartment holds a 9-pin connector and 2 UG-1462/U bulkhead coax jacks.

Special techniques are used to provide the required 120 db of isolation between the reel compartment and the outside. The electronics container is carefully machined to eleminate leaky seams and provide a close tolerance between the sides of the container and the two cover plates. The cover plates are fastened by means of machine screws spaced at 0.5 inch intervals around the perimeter. Compartments separated by a solid wall house the antenna reel and electronic circuits. All wiring from the circuits to the motor, limit switches, and other electro-mechanical parts is twisted and double shielded within the reel compartment. Leads from the electronic circuits to the multi-pin connector (command, power, etc). are RF filtered with flight-approved EMI suppression feedthrough filters (Erie 1200-700 style). A solid wall in the electronic circuits compartment separates the circuits from the multi-pin connector. The feedthrough filters are mounted in this wall. With the double filtering provided by the shielding within the reel compartment and the suppression filters to the multi-pin connector, isolation up to 120 db can be obtained.

The feed end of the antenna is connected to a slip ring mounted on the reel. Two sets of multiple gold-plated spring contacts connect with the slip ring. These contacts are connected in parallel with the coaxial jacks on the rear cover and RF test jack (UG-1462/U) on the front of the unit. When the antenna is partially deployed, the total capacitance with respect to ground of the jacks, wiring, two sets of finger contacts, slip rings, and antenna feed wire is approximately 30 pf.

2.1 MECHANICAL DESIGN

The external configuration was defined by the IMP H & J mechanical interface documents in terms of maximum allowable dimensions (Figure 2-3). Since capacitance to case is critical, the maximum allowable dimensions were used and the internal components were arranged to provide maximum clearance between the antenna conductor and the metal case.

The antenna conductor (wire) originally selected was 7 twisted strands of 0.007 cadmium bronze. This material performed satisfactorily, however, testing established that the breaking strength was slightly under 30 pounds, which did not offer sufficient safety margin. An alternate cable, with the same strand size, made of type 305 stainless steel was procured and was the final material used. Some of the properties of the cable are:

1. Non magnetic.
2. 1/2 grams/ft (approximately)
3. 70 lbs breaking strength.

A coating of extruded FEP teflon 0.005 inch thick was applied to the stainless steel conductor to insulate the antenna from plasma effects in the vicinity of the spacecraft. This material was applied by HAVEG Industries to the basic cable. This material performed well; however, the coating was extremely vulnerable to mechanical damage in handling. Several design modifications were made during the testing program to alleviate stresses imposed directly upon the insulation.

NOTES, UNLESS OTHERWISE SPECIFIED
1. ALL DIMENSIONS ARE FOR REFERENCE ONLY.

REVISIONS			
SYM	DESCRIPTION	DATE	APPROVED
A	RF CONNECTORS WERE UG 1464/U, ELEC CONN. WAS 55 PIN	1-22-72	
B	RELOCATED CONNECTORS ON TOP COVER. ADDED RF CONN PART NO. & DIMS.	6-14-72	
C	ADDED BOTTOM VIEW	6-19-72	

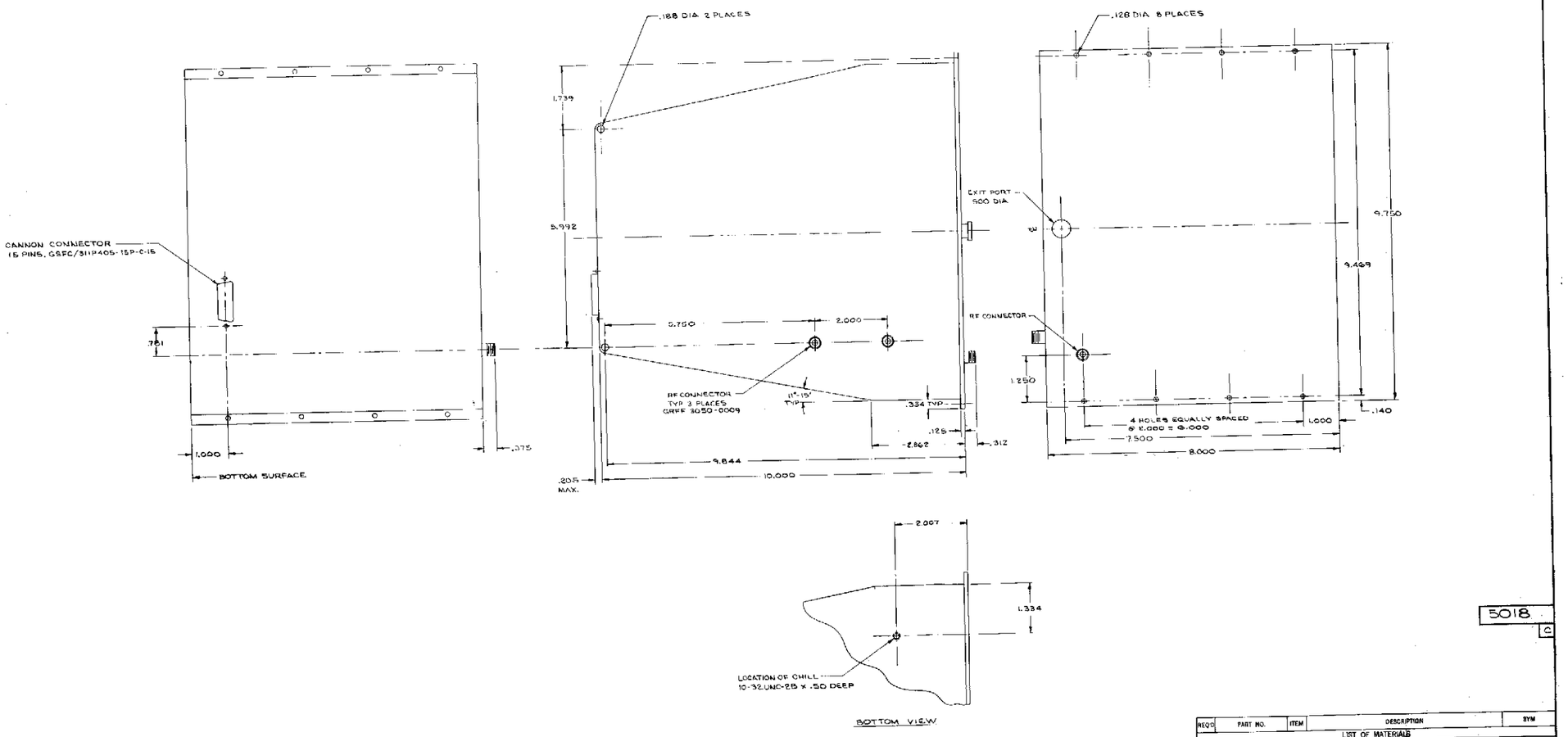

5018 C

REQ'D	PART NO.	ITEM	DESCRIPTION	SYM
			LIST OF MATERIALS	

UNLESS OTHERWISE SPECIFIED
2 PL TOL 3 PL TOL ANGLES
COMMERCIAL PUBLISHED TOLERANCES SHALL APPLY TO SIZES OF WIRE, SHEET, STRIP, ETC. FROM RAW MATERIAL REFERENCE. PLASTIC PARTS MUST FIT GAGES AND MEET SPECIMENS COLLAPSED AFTER PLATING

DRAWN BY D. MACKENZIE — DATE 1-12-72
CHECKED
ENGINEER — 1-25-72
APPROVED
APPROVED
MATERIAL
FINISH
DO NOT SCALE DWG.
NEXT ASSY USED ON

GSFC GSFC AEROSPACE RESEARCH COLLEGE PARK, MARYLAND

OUTLINE DRAWING
BFM ANTENNA
IMP J

CODE IDENT NO. 08141 — SIZE E — 5018 — SCALE 1/1 — SHEET 1 OF 1

PULLOUT FRAME 1

PULLOUT FRAME 2

Appendix A contains a brief analysis of thermal consideration which led to the choice of the FEP coating.

As shown in Figure 2-1 the antenna conductor is stored on a hollow drum with a single helical groove in which the conductor is laid.

As the drum is rotated a traveling nut-which engages this same thread, moves along the axis of the drum, carrying a wire guide which dispenses or stores the conductor depending on direction of drum rotation.

A hysteresis synchronous motor operates at 8000 RPM driving a worm and gear reduction and spur gear train. The total gear reduction is 1440:1 and yields an antenna deployment rate of slightly over 0.11'/second. The worm and gear pair is included for a large velocity reduction and to act as a brake to prevent centrifugal force from deploying the antenna.

All gears including the worm were lubricated with dry molybdenum disulphide in a resin binder Electro Film #4306. Performance of this lubricant was excellent on the aluminum spur gears. On the stainless steel worm-bronze gear pair, the lubricant was inadequate under low temperature (-20^{o} C) vacuum environment. An alternate lubricant (Braykote 803 with 5% MoS_2) was applied to the worm and gear. In the heavily loaded operation this grease was removed by the shaving action of the worm and a lubricant loaded brush was added to re-lubricate the surfaces. It is felt that the major cause of the lubrication problem may well be decreased gear center clearance caused by differential contraction between of the magnesium housing, stainless steel worm and bronze gear.

Various types of motors were evaluated. Among these were: D. C. motors and Permanent magnet and variable reluctance stepper motors, and A. C. Motors.

D C motors have the advantage of being driven directly from the 28 volt supply without interface driving circuitry. Futhermore, high speed d c motors are capable of high efficiency operation. However, when the other parameters and characteristics of a d c motor are investigated several serious defficiencies are noted. First, the speed of the d c motor (without governor) is a function of applied voltage and torque, thus, good speed control and motor to motor tracking are difficult to obtain. Of course, the speed could be precisely controlled by resorting to one of various servo closed loop control techniques, however, this solution requires more complex electronics which inturn considerably lowers the overall efficiency and reliability. Mechanical centrifugal governors which can be packaged within the motor can also be used to achieve speed accuracies of 1 or 2%, however, this approach requires a set of electrical contacts which are continuously breaking the inductive load of the series motor winding. This approach was rejected for reliability reasons.

The reliability of a high quality d c motor is almost entirely dependent on the wear characteristics of the brushes and commutator. Brush wear is caused by mechanical wear with the commutator and electrical erosion caused by electrical arcing. In a totally enclosed motor, the brush wear particles are contained within the motor frame. As a result, these fine particles often find their way to the motor bearings causing premature bearing failure. Futhermore, outgassing in a vacuum environment may cause a film formation on the

motor commutator which can create motor starting problems. The commutator arcing problem also creates several electrical RFI problems which demands exotic RFI filters on the dc power lines.

Stepper motors are driven by sequentially energizing sets of stator windings. The motor shaft is driven as the stator windings are commutated. The number of steps per revolution and thus the angle of rotation per stop is a function of the number and orientation of the motor windings, and in some cases, the winding excitation sequence. The stepping motor windings are energized by a drive circuit which is in turn controlled by switching logic. Motor rotation speed is a direct function of the pulse generator frequency driving the switching logic. Since the pulse generator frequency is easily controlled, the motor speed can be set precisely and held to within 1% over the temperature range using a multivibrator frequency source. Variable reluctance and permanent magnet stepper motors are the two most common types. The variable reluctance motor has the advantage of very low stray magentic field and has a stepping angle of 15° or less. A permanent magnet stepping motor has a slightly higher external magnetic field and normally has a stepping angle of 45° or 90°. The PM motor also exhibits a detent torque with windings de-energized. Due to the greater stepping angle and the ability to drive the motor windings alternately in a push-pull sequence, the efficiency of a PM motor is more than that of a variable reluctance motor. The efficiency of a PM stepping motor, however, is poor when compared to other motor types. The power required by the stepping motor is essentially independent of motor torque, the efficiency at pull-out torque is in the low 20% range for the best PM stepping motors. The Request for Proposal, however, requires a 100% of worst case torque safety factor, therefore, the motor will at worst case torque be operating at a 10% efficiency. Of course, as the torque decreases from worst case, the efficiency becomes even lower.

Although a stepping motor could be made to operate within the 21 watt power limit, the feasibility of using a synchronous motor was investigated. Selected motor can produce a theoretical efficiency of almost 50% at the pull-out torque point and an efficiency of over 30% at the worst case design torque point. This motor has no brushes, and precisely locks to a 40 Hz drive frequency. The hysteresis synchronous motor starts by the hysteresis losses induced in the hardened-steel rotor by the revolving field of the motor winding. Its smooth rotor frees the motor of magentic pulsating resulting from pole saliency of slots, and is therefore much quieter and freer from vibration than a reluctance synchronous motor. Because there is no cogging, smooth and uniform starting conditions results. The hysteresis synchronous motor can synchronize high inertial loads, and can pull into synchronization a torque almost equal to the pull-out torque of the motor. The motor pulls into synchronism with the drive voltage frequency because of the retentivity of the rotor. The synchronous motor drive frequency need not slew up to the final drive frequency as would be required if the stepping motor were operated in its slew range. The synchronous motor selected has a motor performance which is specified by curves shown in Figures 2-4a and 2-4b. The worst case operating torque point was selected at approximately one-half of the motor pull-out torque point. As shown in Figure 2-4a, the locked rotor torque of the motor is approximately 35% greater than the pull-out torque of the motor providing an additional safety margin.

Each end of the two motor windings is driven by a push-pull solid state current driver as shown in Figure 2-5. The drivers are controlled by an electronic commutator which drives the two windings 90^{o} out of phase.

The efficiency of a hysteresis synchronous motor is decreased somewhat by the presence of drive harmonics; therefore, a proprietary drive technique was developed which drives the winding by a waveform optimized for efficiency. Appendix B contains a brief analysis of this technique.

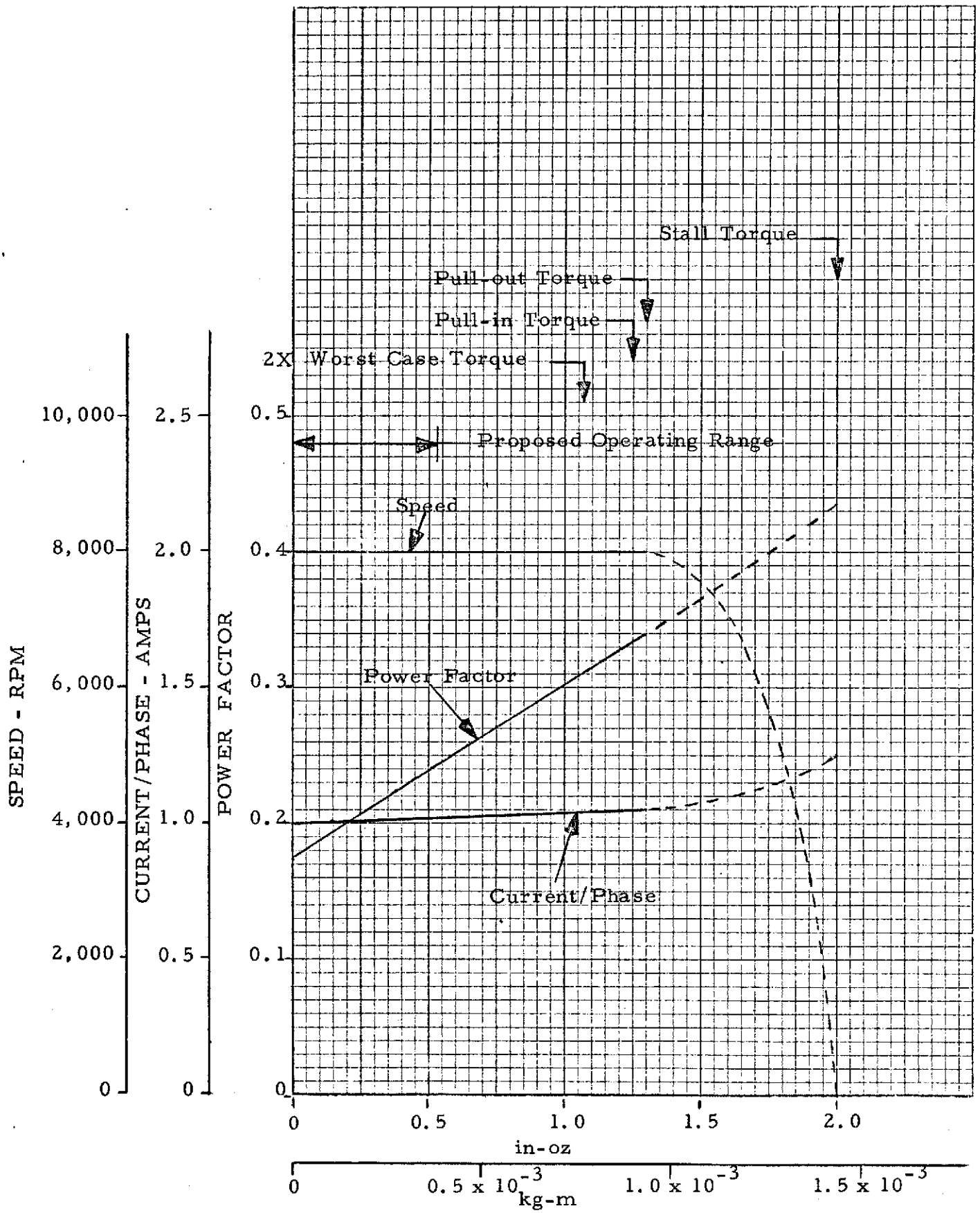

FIGURE 2-4a

KEARFOTT TYPE CT20174024 HYSTERESIS SYNCHRONOUS MOTOR PERFORMANCE CURVES

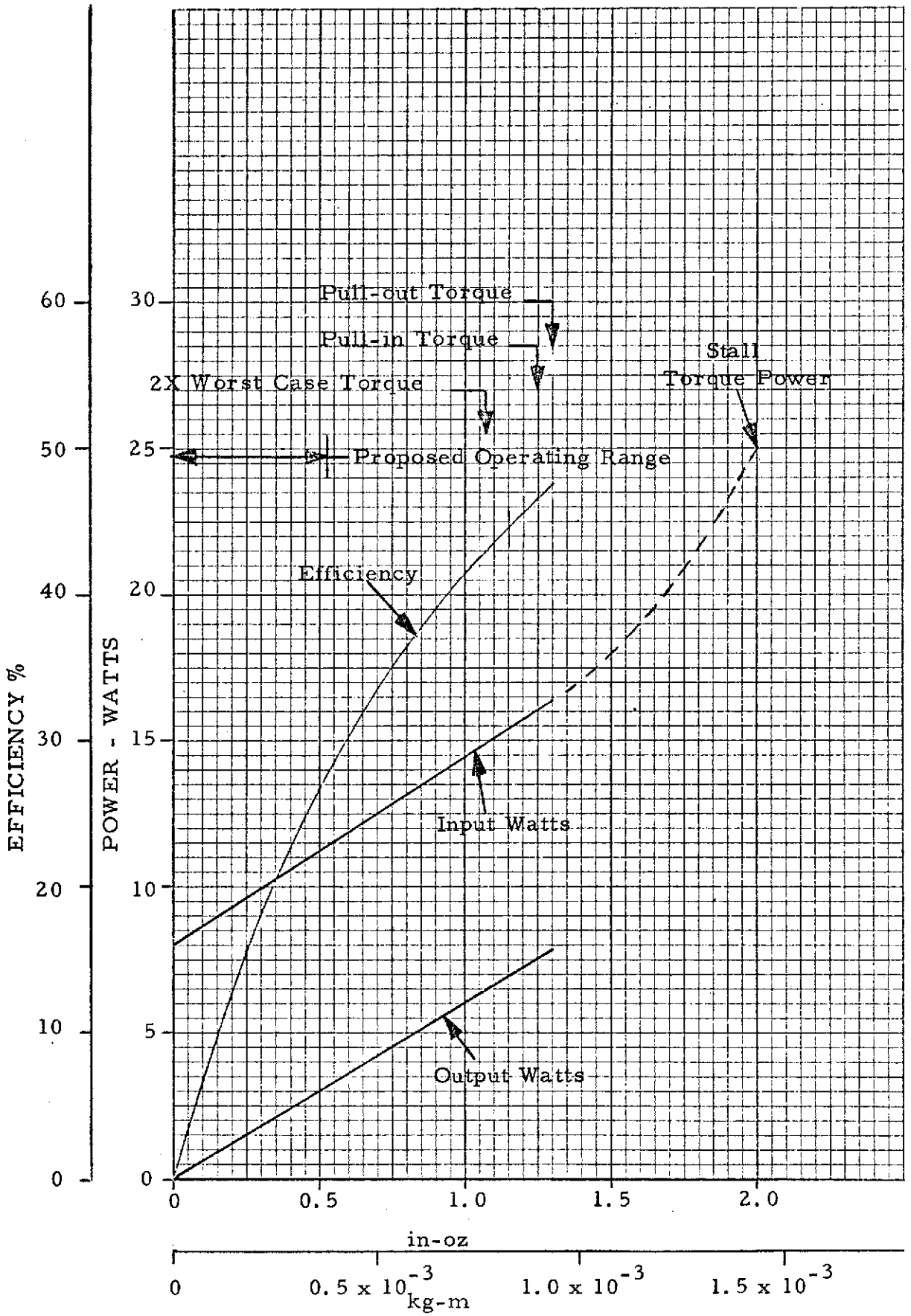

FIGURE 2-4b

KEARFOTT TYPE CT20174024 HYSTERESIS SYNCHRONOUS MOTOR PERFORMANCE CURVES

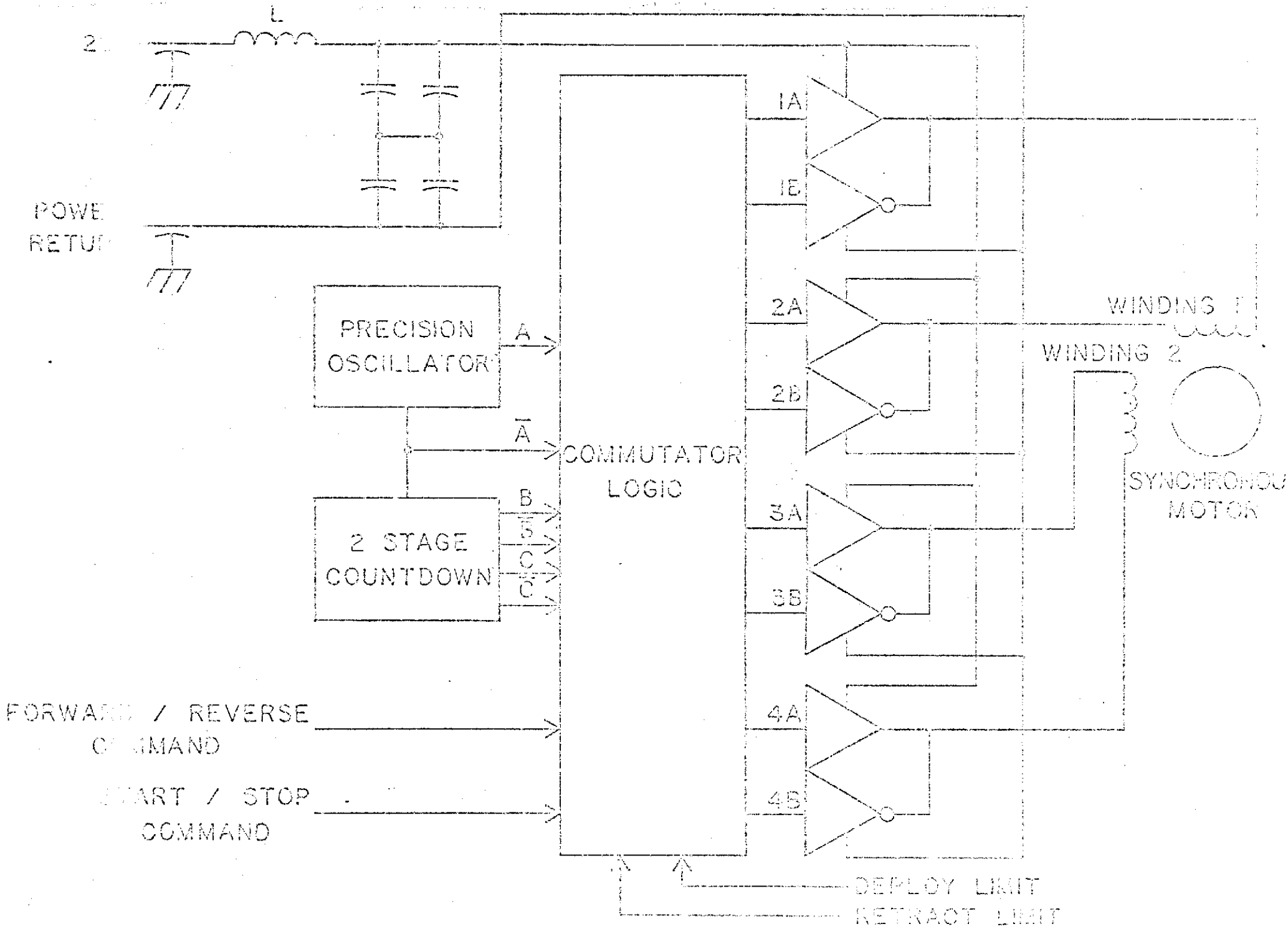

FIGURE 2-5 MOTOR DRIVER BLOCK DIAGRAM

2.2 ELECTRONICS

Three electrical circuits are used in the EFM antenna module. Each of these circuits has independent ground returns to spacecraft ground to prevent interference between circuits. The operation of these circuits is discussed in this section. (Reference Figure 2-6)

Figure 2-7 illustrates the Electrical Interface of each antenna with the spacecraft.

2.2.1 Antenna and Feed Circuit

This circuit consists of the 200 ft antenna wire which is attached at the feed end to a slip-ring mechanism on the plastic storage drum. The last 150 feet of antenna wire to be deployed is insulated to prevent interference from extraneous signals near the spacecraft. A bifilar brush assembly connects the antenna feed to 2 coaxial connectors for output to the experiment preamplifiers. The antenna feed is also connected to a microswitch which shunts the antenna with 1000 Megohms when the antenna is in the fully retracted position only. The antenna circuit has approximately 60 pf of shunt capacitance to frame while it is stowed on the plastic drum. This capacitance decreases to less than 30 pf when the antenna is fully deployed. Antenna shunt resistance to frame is greater than 10,000 megohms. The storage compartment is designed to provide greater than 105 db isolation (50-ohm reference) from the motor driver and telemetry circuits.

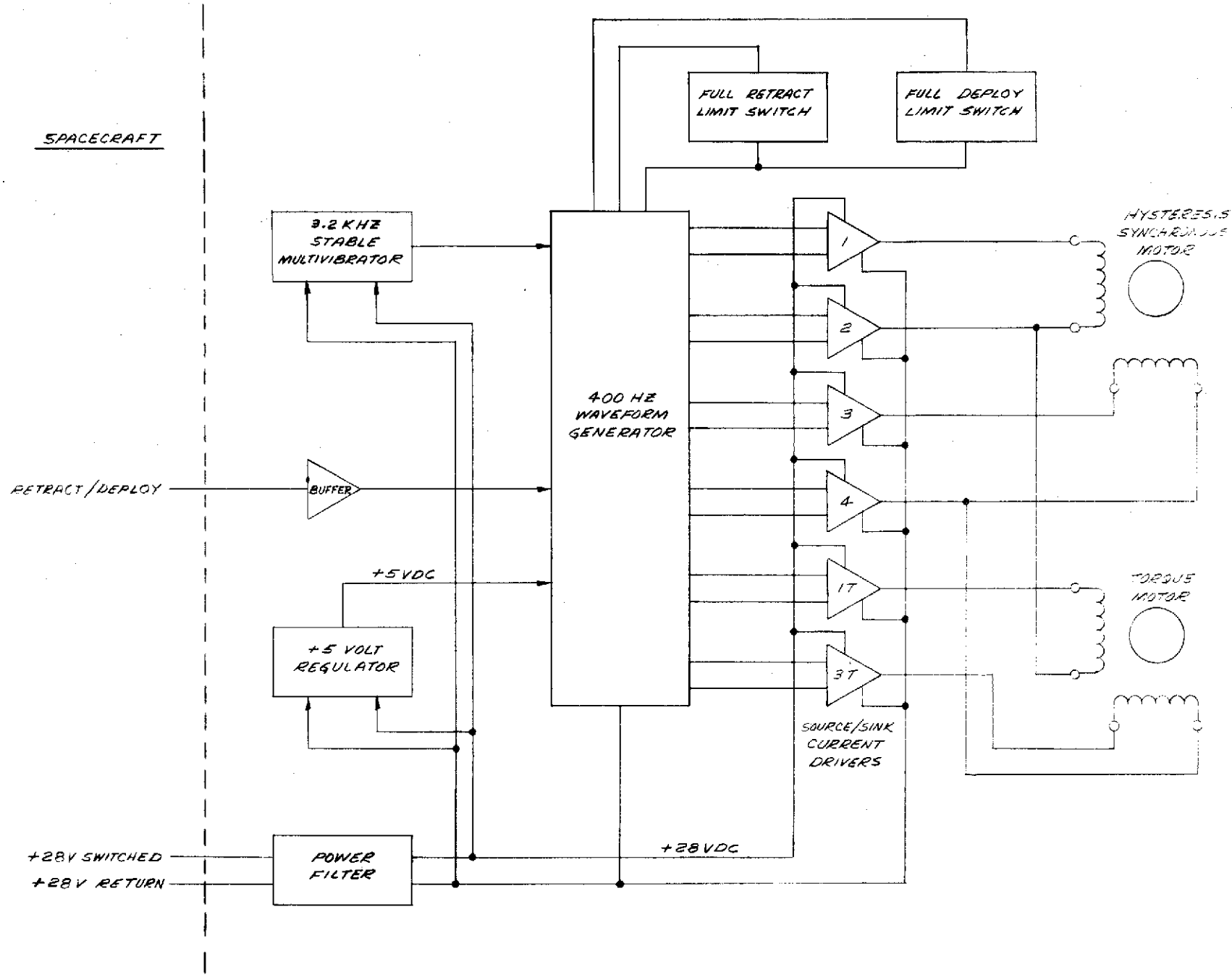

FIGURE 2-6 BLOCK DIAGRAM — EFM ANTENNA MECHANISM DRIVE CIRCUIT

REVISIONS			
SYM	DESCRIPTION	DATE	APPROVED
B	REDRAWN WITH CHANGES	8-2-72	

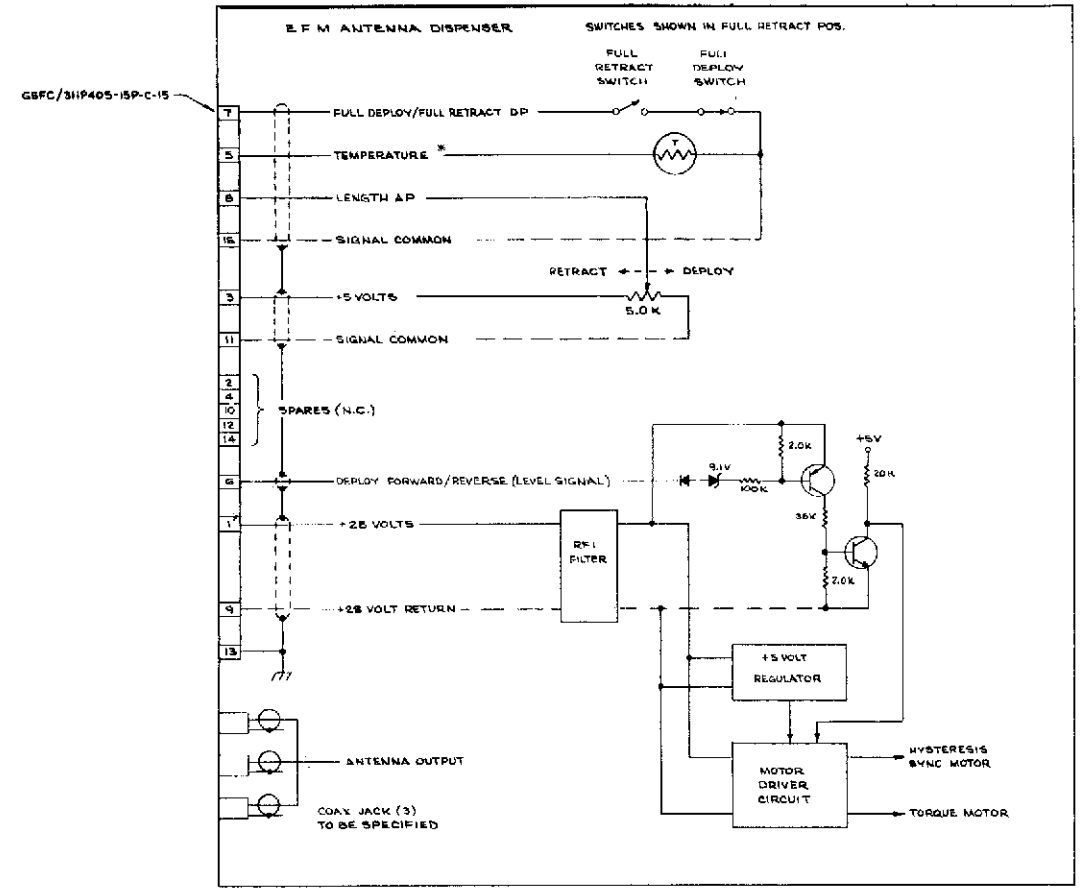

* ONLY IF DIRECTED BY GSFC.

4044
B

REQ'D	PART NO.	ITEM	DESCRIPTION	SYM

LIST OF MATERIALS

UNLESS OTHERWISE SPECIFIED 2 PL TOL 3 PL TOL ANGLES	DRAWN BY TD MAKEMENTER	DATE 7-27-72	EMR Schlumberger — EMR AEROSPACE SCIENCES COLLEGE PARK, MARYLAND
COMMERCIAL PUBLISHED TOLERANCES SHALL APPLY TO SIZES OF BAR, ROD, WIRE, SHEET, TUBE, ETC. WHEN MARKED WITH AN ASTERISK (*). PLATED PARTS MUST FIT GAGES AND MEET SPECIFIED TOLERANCES AFTER PLATING.	CHECKED		EFM ANTENNA DISPENSER IMP J INTERFACE
	ENGINEER G. MACKAY	8-2-72	
	APPROVED		
MATERIAL	DO NOT SCALE. DWG.		CODE IDENT NO. 08141 — SIZE D — 4044
FINISH			SCALE — SHEET OF
4020 NEXT ASSY	USED ON		

2.2.2 Motor Driver and Control Circuit

This circuit is designed to drive a 400 Hz, 2-phase hysteresis synchronous motor and a 400 Hz, 2-phase torque motor from a +28 volt power source. The hysteresis synchronous motor drives the antenna drum at a constant rate during deployment while the torque motor maintains a tension on the antenna wire at the deployment post. During retraction the hysteresis synchronous motor is reversed to retract the antenna at the same rate as deployment. The torque motor is disabled during retraction. The motor direction is controlled by the DEPLOY FWD/REV input from the spacecraft. When this line is connected to the 28VDC return the motors will deploy when the +28 volts power is applied. Deployments will continue until either the power is removed or the antenna is fully extended (200 ft) and a limit microswitch commands the control circuit to disable the motors. The antenna is retracted by opening the DEPLOY FWD/REV control line. When the +28 volt power is applied the hysteresis synchronous motor retracts the antenna until either the power is removed or the antenna is fully extracted and a second limit microswitch commands the control circuit to disable the motor. The +28 volt power should be turned off after either full deployment or full retraction to conserve power since the control circuitry remains powered when the motors are disabled by either limit switch.

Source-Sink Current Drivers

The end of each motor winding is connected to a source-sink current driver which can select the +28 volt power, the +28 volt return, or neither. The source switch at one end of a winding operates in conjunction with the sink switch at the other end to drive current in one direction through the motor winding during one-half of the power cycle. During the second half of the cycle the other source and sink operate to drive current through

the winding in the opposite direction. Saturated current switches are used to prevent excessive heating in the driver circuits. The second winding of the motor operates similarly except that the power cycle is phased either 90 or 270 degrees with respect to the first winding to drive the motor either clockwise or counterclockwise. The torque motor uses a separate pair of driver switches at one end of each winding and shares a driver switch pair at the other end of each winding with the hysteresis synchronous motor. In this way the separate torque driver switches are disabled during retraction and the torque motor is inoperative.

Motor Control Circuit

This is a LPTTL logic circuit whose function is to provide enable signals for the source sink current drivers. The circuit is powered by the +28 volt power through a +5 volt regulator. A delay circuit is included in the logic to hold the motors off for the first 50 milliseconds after the +28 volt power is applied to allow the logic to stablize and function normally. The logic circuit is controlled by the DEPLOY FWD/REV control signal and the full deploy and full retract limit switches. The source-sink switch signals generated by the logic are modified square waves whereby the source switch is enabled for only 3/8 of a cycle instead of the full 1/2 cycle to reduce the harmonic content of the motor winding currents and thereby increases the efficiency of the motor. A full discussion of the proprietary technique is included in appendix B of this report.

Stable Oscillator

A 3.2 khz free running multivibrator is used to provide timing fo the control logic. This circuit is designed to operate within ± 1 percent of the nominal frequency since its stability determines the stability of the 400 Hz motor drive power and antenna deployment rate. Any two antenna modules on the spacecraft will deploy or retract within ±2 percent.

2.2.3 Telemetry Circuit

The EFM antenna module has a 20-turn 5 K linear potentiometer which is driven by the antenna wire during deployment or retraction. When the antenna is fully retracted the potentiometer output is within one turn of maximum voltage and when the antenna is fully extended the potentiometer output is within one turn of zero voltage. A +5VDC signal from the spacecraft is used as a reference signal. The LENGTH AP output signal is calibrated in respect to antenna length over the full 0 to 200 foot extension range.

Separate full-extend and full-retract limit switches are wired in series to a FULL DEPLOY-FULL RETRACT DP so that the circuit is open only when the antenna is either fully extended or fully retracted.

Both the LENGTH AP and the FULL DEPLOY-FULL RETRACT DP signals are furnished to the spacecraft telemetry system.

2.3 TESTING

The mechanisms were subjected to an environmental test program in order to qualify the antennas for flight use on the IMP J Spacecraft. The program was based on portions of the Environmental Test Specification for the Interplanetary Monitoring Platform, IMP H & J sybsystems, S-320-IMP-6.

A spin table equipped with slip rings was fabricated and used to verity the mechanism's ability to extend and retract at various initial spacecraft spin rates. Tests were performed at spin rates from 100 RPM to 60 RPM before and after the mechanisms were exposed to the vibration environment.

Operational tests were performed before and after the environmental test program. These consisted of full extensions and retractions into a take up device that created a tension profile which simulated the centrifugal force expected during deployment in orbit.

3.0 NEW TECHNOLOGY

In accordance with the definitions in NHB2170.1, "New Technology Reporting", this contract has been considered as a Type II Project. Nearly all of the scientific effort has been in the fields of electrical and mechnical engineering. Work has included subsystem design, design study, system development, theoretical analysis, specification evaluation and design "trade-off" analysis.

During the performance of the project each of the engineers and technicians assigned was periodically reminded of the importance both EMR and NASA place on the disclosure of new technology. On a regularly scheduled basis, such disclosures were reviewed by the New Technology Review Committee consisting of the managers of each department at EMR and of the General Manager. This committee then decided upon the disposition of each disclosure.

The proposal prepared by EMR resulting in the award of this contract described in detail a unique motor drive circuit. Prior to contract award, this circuit was evaluated on a breadboard basis to assure feasibility. During performance of the contract the circuit was implemented in final form, tested and documented. A description and analysis of this circuit provided in Appendix B to this report.

Based on a thorough review, this circuit constitutes the only disclosure of new technology related to this contract.

APPENDIX A

Antenna Thermal Considerations

The antennas will consist of four wires 0.021 inches in diameter and 200 ft. long each, extending radially outward from the spacecraft in a plane perpendicular to its axis of spin. These wires will be extended from reels mounted in the spacecraft which may be required to retract the wires under some circumstances. The outer 50 ft. of each wire will be uninsulated, but the inner 150 ft. will have an insulating covering of 5 mil Teflon.

The major thermal problems which must be considered are the following:

1) The maximum temperature reached by the wire must not degrade the insulating coating or excessively reduce the tensile strength of the wire.
2) The minimum temperature reached by the wire at a time when it is being reeled in or out must not be low enough to cause brittleness of the wire or its insulating covering.
3) The temperature difference between the sunlit side of the wire and the opposite side must not be large enough to produce appreciable curvature of the antenna.

The first two of these problems can be examined by calculating the steady state temperature limits of the wire. Only the condition of the spacecraft in full sun will be considered. (It is assumed that the antennas will be neither deployed nor retracted while the spacecraft is in shadow.)

The steady state temperature of a long thin wire in full sun depends upon its surface solar absorptance α_s, its emittance ϵ, and its orientation relative to the sun.

$$T^4 = \frac{A_s \sigma S \alpha}{A \epsilon}$$

S = solar constant = 1.36×10^{-1} watts/cm^2

σ = Stephan Boltzmann constant = 5.67×10^{-12} watts/cm^2 deg^4

α_s = integrated solar absorptance

ϵ = emittance

A_s = projected area perpendicular to solar radiation

A = effective emitting area

For the case of the spacecraft axis parallel to the spacecraft-sun line, the wires will have a maximum projected area of $A_s/A = \frac{1}{\pi}$. As the spacecraft axis is rotated away from the spacecraft-sun line, the value of A_s/A will decrease to a minimum value of $A_s/A = 2/\pi^2$ at 90°. Here the sun line is parallel to the plane of the antenna wires. The portion of the wire for which the temperature is critical, however, is the part which is flexing as the antenna is being deployed or retracted. This portion is very close to the spacecraft body, and so will be shadowed up to half of the time. Thus the meaningful minimum value of $A_s/A = \frac{1}{\pi^2}$. These values of A_s/A are averages over a full revolution of the spacecraft about its axis. It is assumed that this rotation is rapid enough that temperature oscillations over a half revolution are not significant.

Some temperature limits are calculated below using $T^4 = (2.4 \times 10^{10}\ \text{deg}^4)(A_s/A)(\alpha_s/\epsilon)$ for a variety of wire surface materials.

Material	α_s	ϵ	α_s/ϵ	T@ $A_s/A = \frac{1}{\pi}$	T@ $A_s/A = \frac{1}{\pi^2}$
evaporated gold	.2	.02	10	525°K	395°K
evaporated aluminum	.08	.02	4	418°K	315°K
black paint or black teflon	.9	.9	1	296°K	222°K
clear teflon over gold	.2	.8	1/4	209°K	173°K
clear teflon over aluminum	.08	.8	1/10	166°K	125°K
oxidized bronze	.5	.5	1	296°K	222°K
stainless steel	.46	.23	2	352°K	264°K

These temperatures were calculated for the steady state, considering only radiative heat transfer between the sun, the wire and space. Radiative and conductive heat transfer to the spacecraft will have some influence on the wire temperature, particularly on the near portion, bringing the wire temperature closer to the spacecraft temperature.

The materials to be used for the antenna wires and for the insulated covering can be chosen so that their values of α_s/ϵ will give operating temperature limits within which their mechanical properties remain satisfactory.

The third thermal problem is determination of the distortion of the wire due to unsymmetrical solar heating. An exact calculation of this effect would be very tedious, but an order of magnitude approximation can quickly show that the resulting curvature is negligible. For this approximate calculation, consider the wire to be of square cross section of thickness d, with the entire solar heat load incident on one face, and reradiated to space by the opposite face. The heat absorbed per unit length will be $S\alpha_s d$. If we consider this total heat flux as transmitted the distance d to the other face through a medium of conductivity K, the temperature difference ΔT between faces will be

$$\Delta T = \frac{1\, d^2\, S\alpha_s}{K\, 1\, d} = \frac{d\, S\alpha_s}{K}$$

taking $d = 0.021$ inch $= 5.33 \times 10^{-2}$ cm

$$K = 0.1 \ \frac{\text{cal}}{\text{cm deg C sec}} = 0.42 \ \frac{\text{watts}}{\text{cm deg C}}$$

$$\alpha_s = 1.0$$

$$S = 136 \times 10^{-3} \text{ watts/cm}^2$$

$$\Delta T = \frac{(5.33 \times 10^{-2}\text{cm})(.136 \times 10^{-3}\ \text{w/cm}^2)(1.0)}{0.42\ \text{watts/cm deg C}} = 1.7 \times 10^{-2} \text{ degree C}$$

This approximation has been calculated as a maximum value of ΔT. If we assume a thermal expansion coefficient of 1.0×10^{-5} per degree C (typical

for stainless steel), we have a differential expansion of 1.7×10^{-7} between the two sides of the wire. If the wire were not under tension, this would correspond to a radius of curvature of $R = \frac{0.021 \text{ inch}}{1.7 \times 10^{-7}} = 1.2 \times 10^{5}$ inches $\approx 10^{4}$ ft

Thus even neglecting the straightening effect of centrifugal force, the thermally induced curvature of the wire is not significant.

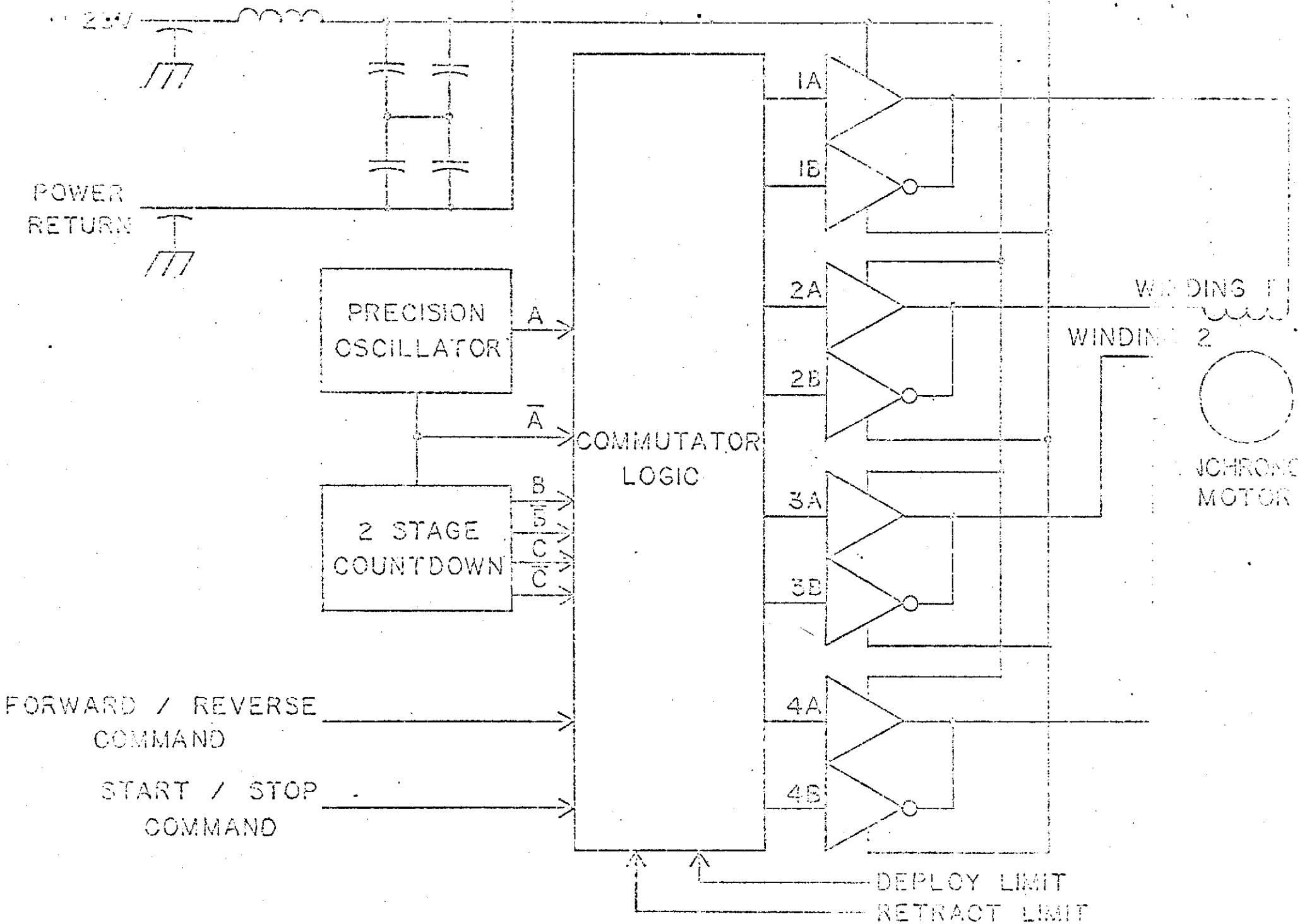

FIGURE 4 MOTOR DRIVER BLOCK DIAGRAM

APPENDIX B

Drive Circuit Analysis

The efficiency of a hysteresis synchronous motor is decreased when the sinusoidal motor drive is replaced by the square - wave drive obtained from a DC power source. To improve the square - wave efficiency EMR has developed a proprietary modified square-wave drive technique whereby the positive and negative parts of the drive waveform are separated by an "off" period whose width is set to optimize the amplitude of the fundamental frequency.

The general waveform which is to be optimized is shown in figure 1. The Fourier series representation of this waveform is:

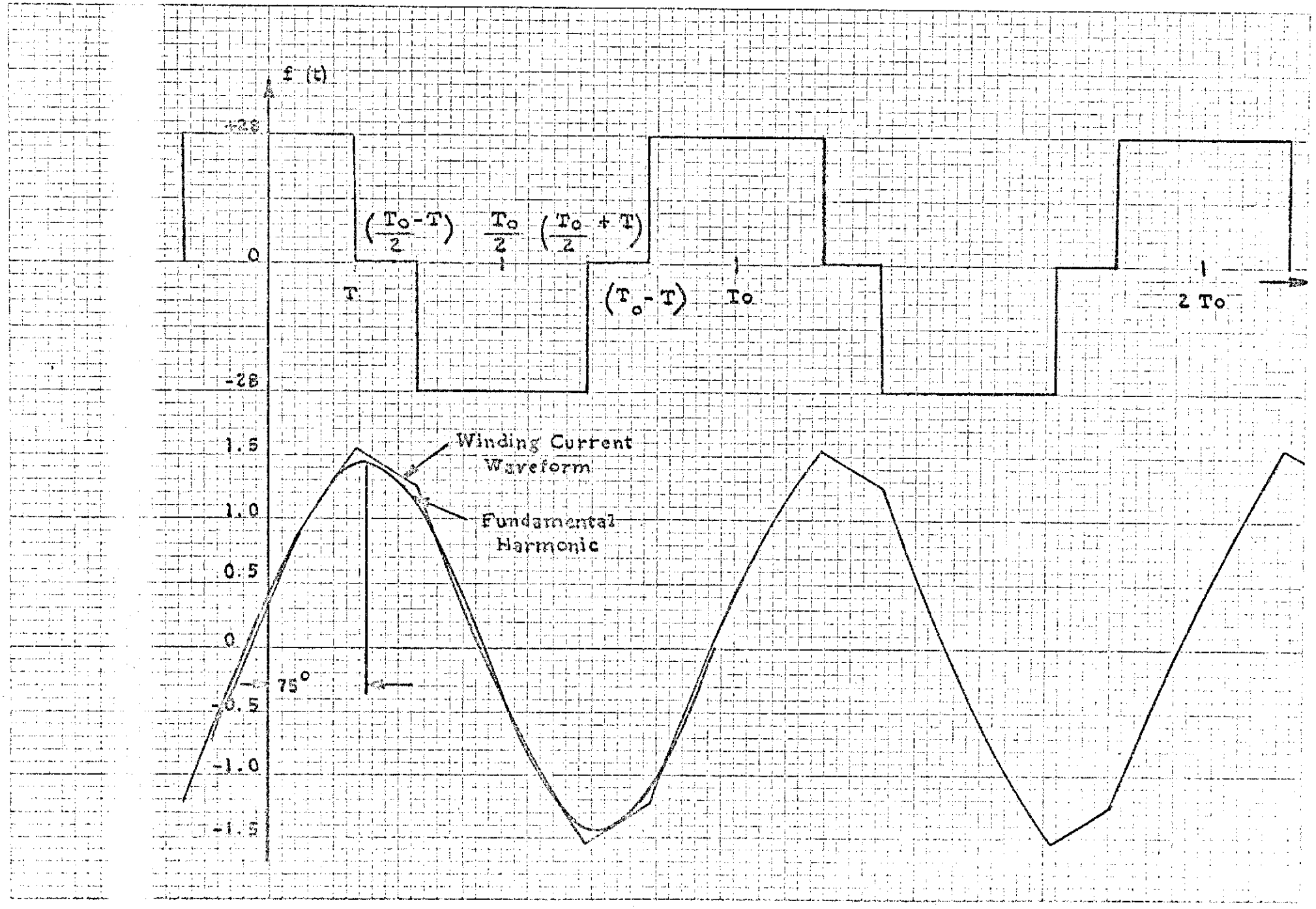

FIGURE 1 WINDING VOLTAGE AND CURRENT WAVEFORMS

(1)

$$f(t) = \frac{4A}{\pi} \sum_{\frac{n+1}{2}=1}^{\frac{n+1}{2}=\infty} \frac{1}{n} \sin\left(2\pi n \frac{T}{T_o}\right) \cos(nwt)$$

For maximum efficiency, it is desirable to choose a value of T/T_o which produces the maximum fundamental rms to input rms ratio.

(2)

$$\eta = \frac{E_{rms}\ (\text{fundamental})}{E_{rms}\ (\text{input})}$$

The rms value of the fundamental can be determined from equation (1).

(3)

$$E_{rms}\ (\text{fundamental}) = 0.707\left(\frac{4A}{\pi} \sin\left[2\pi \frac{T}{T_o}\right]\right)$$

The rms value of the input waveform can be determined by using the root-mean-square intergral.

(4)

$$E_{rms}\ (\text{input}) = \left(4A^2 \frac{T}{T_o}\right)^{1/2}$$

Substituting equation (3) and (4) into equation (2) and simplifying the resulting expression.

(5)

$$\eta = \frac{4}{\pi} \frac{\left(\sin 2\pi \frac{T}{T_o}\right)^2}{\left(2\pi \frac{T}{T_o}\right)}$$

By differentiating the above equation in respect to T and setting the result equal to zero the maximum efficiency point is found to be:

$$\frac{T}{T_o} = .1855$$

and $T = 66.8^o$

At this value of T/T_o, the rms value of the fundamental waveform is 92.28% of the input waveform. This value is compared to a value of 81.05% for a square wave excitation input.

The motor chosen is a size 15, type CT20174024 manufactured by the Kearfott division of Singer-General Precision, Inc. The winding wire size and number of turns are changed so the motor can operate at the prescribed voltage level. The input power and torque characteristics however, remain the same as specified for the 115 volt motor. Curves showing the speed, input power, output power, factor, efficiency and current per phase are shown in Figure 5 and 6 for the proposed motor. This motor will pull into synchronization with the 400 Hz applied voltage waveform within 28 ms after power turn-on at 1/2 pull-out torque. An idealized current waveform was derived for a motor winding with a equivalent circuit represented by a series resistor and inductor. The values of these components were calculated at a torque corresponding to .65 inch-ounces or 1/2 pull-out torque. The current waveform produced by applying a voltage waveform using the above calculated T/T_o ratio is shown in Figure 1. The fundamental of the resultant current waveform is also plotted for comparison. It is observed that the harmonic content is almost negligible. For equal motor performance, the input power to each winding is 6.10 watts when driven from a 400 Hz sine wave source and only 6.124 watts when driven by the proposed waveform at a 400 Hz rate. Less than 1% is lost in efficiency by driving the motor with the proposed voltage waveform. The reason that the efficiency is much higher than the 92.28% figure previously calculated which represents the rms value of the fundamental to rms value of

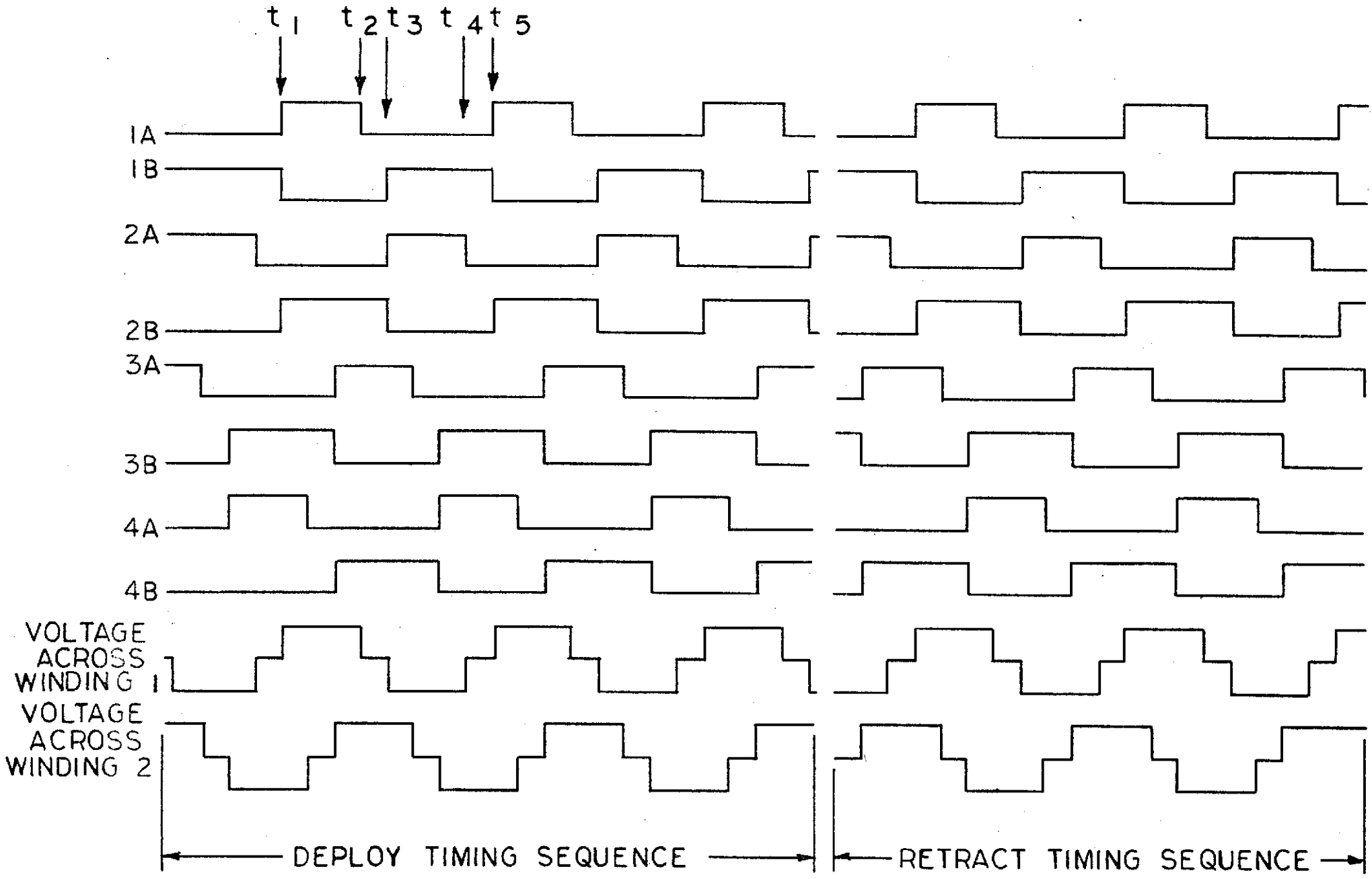

FIGURE 2 DRIVER INPUT WAVEFORMS

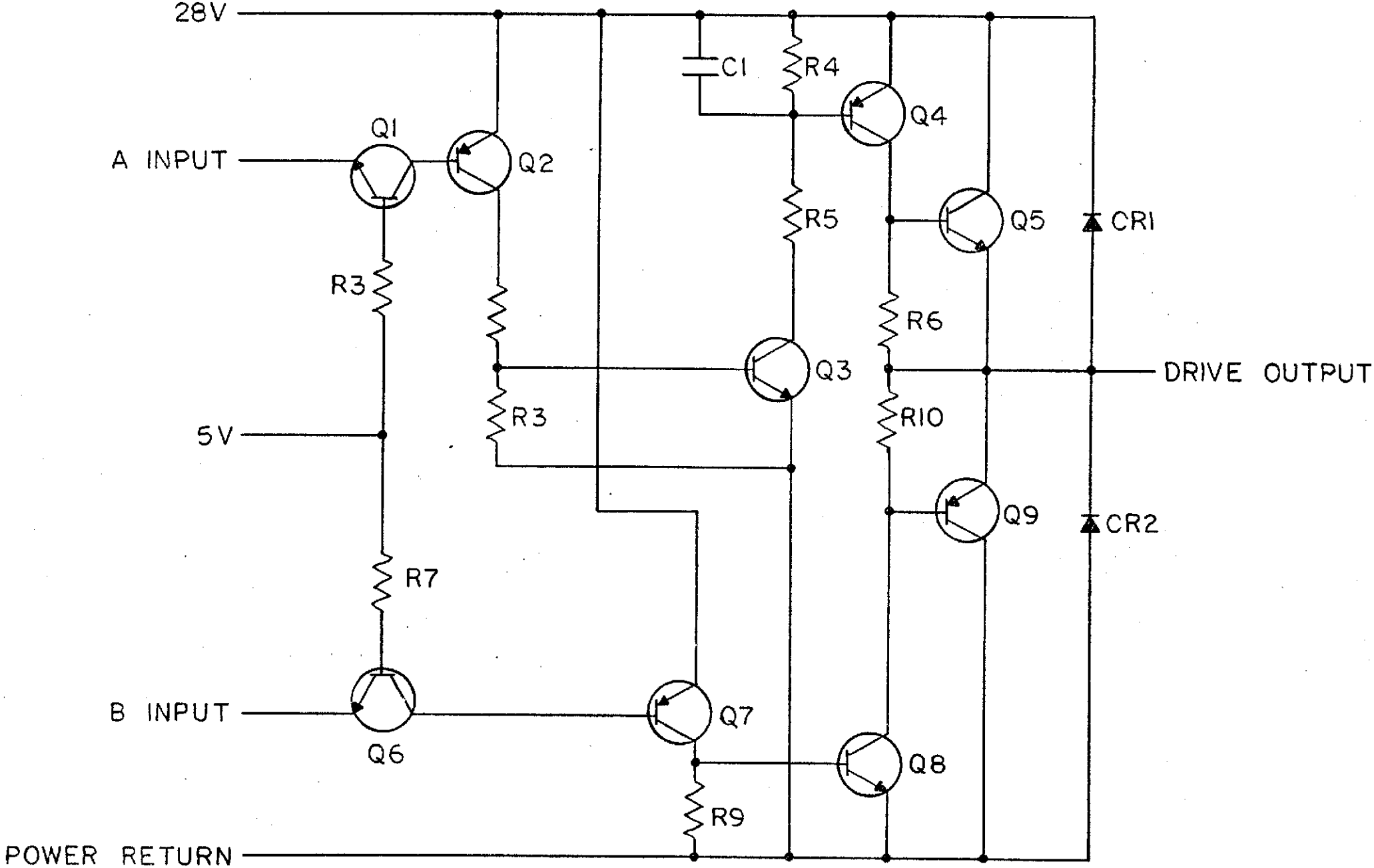

FIGURE 3 TYPICAL DRIVE CIRCUIT

$$\frac{T}{T_o} = .1855$$

and $T = 66.8^o$

At this value of T/T_o, the rms value of the fundamental waveform is 92.28% of the input waveform. This value is compared to a value of 81.05% for a square wave excitation input.

The motor chosen is a size 15, type CT20174024 manufactured by the Kearfott division of Singer-General Precision, Inc. The winding wire size and number of turns are changed so the motor can operate at the prescribed voltage level. The input power and torque characteristics however, remain the same as specified for the 115 volt motor. Curves showing the speed, input power, output power, factor, efficiency and current per phase are shown in Figure 5 and 6 for the proposed motor. This motor will pull into synchronization with the 400 Hz applied voltage waveform within 28 ms after power turn-on at 1/2 pull-out torque. An idealized current waveform was derived for a motor winding with a equivalent circuit represented by a series resistor and inductor. The values of these components were calculated at a torque corresponding to .65 inch-ounces or 1/2 pull-out torque. The current waveform produced by applying a voltage waveform using the above calculated T/T_o ratio is shown in Figure 1. The fundamental of the resultant current waveform is also plotted for comparison. It is observed that the harmonic content is almost negligible. For equal motor performance, the input power to each winding is 6.10 watts when driven from a 400 Hz sine wave source and only 6.124 watts when driven by the proposed waveform at a 400 Hz rate. Less than 1% is lost in efficiency by driving the motor with the proposed voltage waveform. The reason that the efficiency is much higher than the 92.28% figure previously calculated which represents the rms value of the fundamental to rms value of

the input voltage drive is that at the calculated T/T_o ratio the 3rd and 5th harmonics are very small. The 7th harmonic and above see a large coil inductive reactance; therefore, the power dissipated by the harmonics is the above negligible value.

The actual motor commutator is designed with a value of T equal to 67.5°. This considerably simplifies waveform generation since voltage is alternately applied across each winding for periods of $3\pi/4$ radians with zero volts applied between alternate voltage pulses for a period of $\pi/4$ radians as shown in Figure 2. This slight change in T has negligible effect on the previous efficiency calculations. Again, referring to Figure 2 it is seen that the motor is reversed by changing the timing sequency of winding 2 voltage drive waveform. The voltage waveform lags the winding 1 waveform by 90° when the motor is to run in the forward direction and leads the winding 1 waveform by 90° in the reverse direction. A typical drive circuit is shown in Figure 3. Output transistor Q5 is energized applying 28 volts to the winding when the A input is high, and output transistor Q9 is energized which grounds the winding terminal when input B is high. Referring again to Figure 3 with a driver at each end of motor winding 1 as shown in Figure 4, let us consider a winding drive sequence. At time t_1, the A input to driver 1 goes high and the B input goes low which turns on Q5 and turns off Q9 which applies 28 volts to one side of the winding. Capacitor C1 is included in the drive circuit (see Figure 3) which slightly delays the turn-on of Q5 to insure sufficient turn off time of Q9 thus preventing a current through Q5 and Q9 at the transition time. At time t_1, the B input of driver 2 goes high turning on transistor Q9. This produces a 28 volt potential across winding 1 and current goes from the 28 volt supply through Q5 of drive circuit 1, through the motor winding, and through Q9 of drive circuit 2 to the power return line. At time t_2, transistor Q5 of drive circuit 1 is turned off. No transition problem occures at t_2 since Q9 of driver 1 does not turn on until time t_3. During this interval the inductive field of the motor causes current to continue flowing from driver 1 to driver 2 (see Figure 1). This current flows through diode CR2 of driver 1, through

the motor winding, and through transistor Q9 of driver 2. The voltage across the motor winding during this interval is the sum of the voltage drops of CR2 and Q9. At time t_3, transistor Q9 of driver 2 turns "off" and transistor Q5 turns "on" applying 28 volts to the driver 2 side of the motor winding. At time t_3, Q9 of driver 1 is turned "on". At time t_3 (see Figure 1) the forward current through the motor coil still has not decayed to zero. Therefore, since Q9 of driver 2 is turned off, the current continues flowing in the forward direction from ground through CR2 of driver 1, through the motor winding, to the 28 volts supply through diode CR1. The inductive field for a period of time after switching point t_3 is generating power and returning power to the 28 volt supply. At the point the winding current decays through zero, the reverse current is supplied from the 28 volt supply through transistor Q5 of driver 2, through the motor winding, and through transistor Q9 of driver 1 to ground. At point t_4, Q5 of driver 2 is turned off and the reverse current in the t_4 to t_5 interval continues flowing through CR2 of driver 2 and Q9 of driver 1. At time t_5, Q5 of driver 1 turns "on" and Q9 turns off again applying 28 volts to the driver 1 side of the winding. Q9 of driver 2 also turns "on" at time t_5. The reverse current decays through CR2 of driver 2 and CR1 of driver 1 until it reaches zero at which time forward current will again flow through Q5 of driver 1 and Q9 of driver 2. The drive operation of winding 2 is identical except it is made to either lead or lag the winding 1 drive frequency by 90^{o} as shown in Figure 2.

The composite waveform drawing of the current profile of the 28 volt power source is shown in Figure 7. An inductor will be placed in series with the 28 volt line as shown in Figure 4. to smooth current ripple to within the ±125 milliamp requirement of the RFP. Since the lowest frequency of the current ripple is 1600 Hz, the above filtering can be accomplished easily with a small inductor and capacitors which are shown in quad redundant configuration for reliability. In addition, RFI filters will be used to keep the conducted line interference below acceptable limits as well as protecting the internal antenna from interference external to the antenna package.

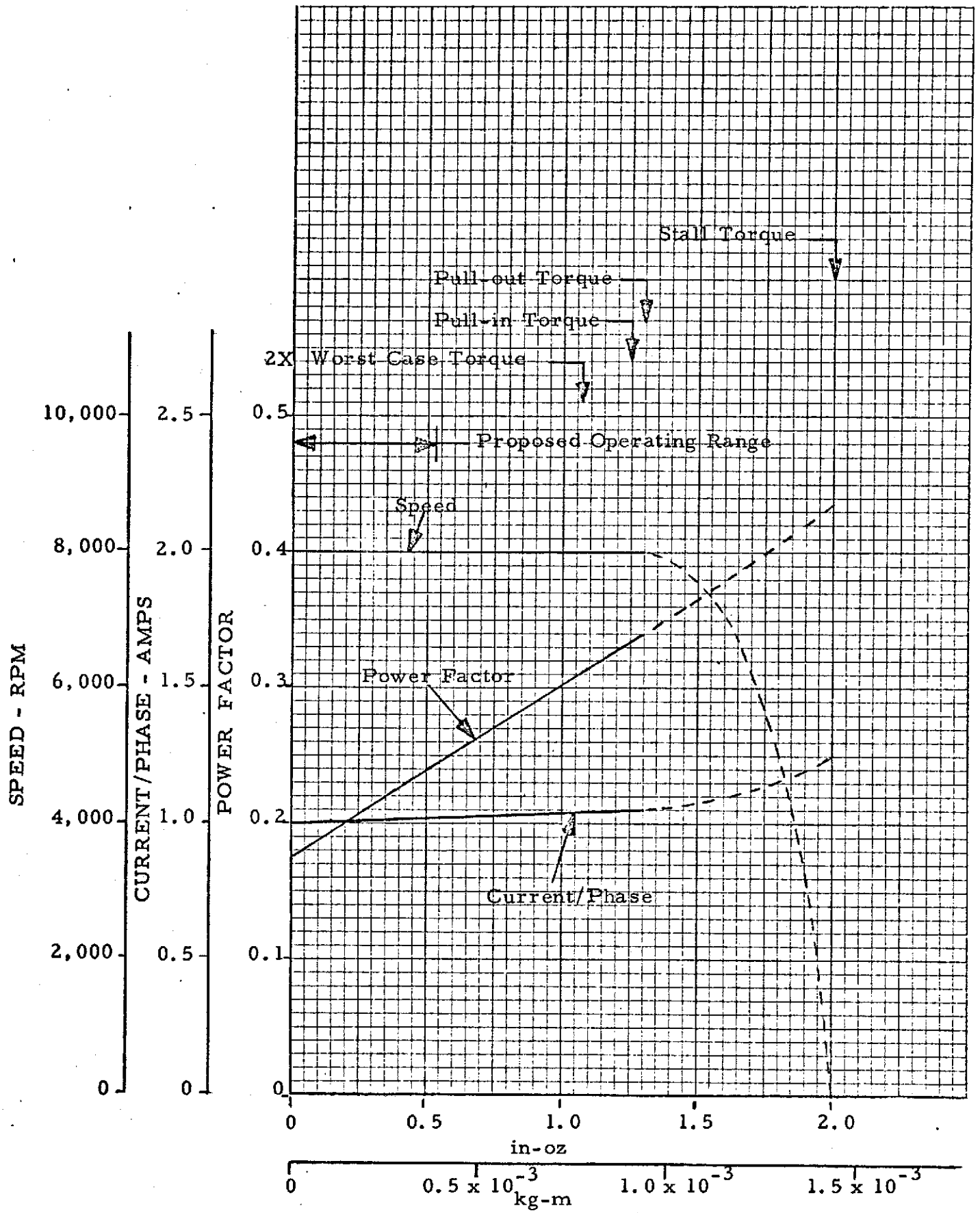

FIGURE 5

KEARFOTT TYPE CT20174024 HYSTERESIS SYNCHRONOUS MOTOR PERFORMANCE CURVES

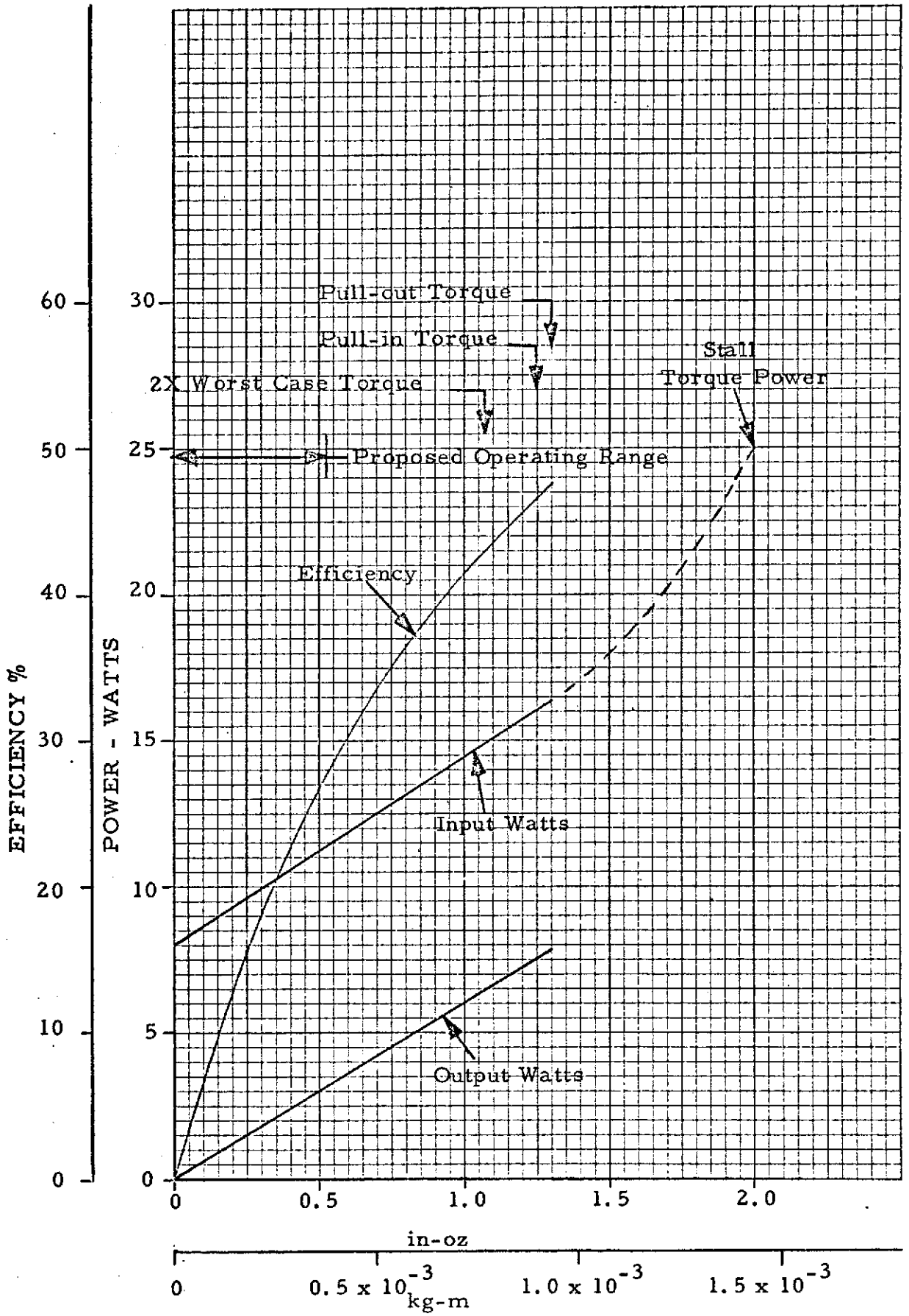

FIGURE 6

KEARFOTT TYPE CT20174024 HYSTERESIS SYNCHRONOUS MOTOR PERFORMANCE CURVES

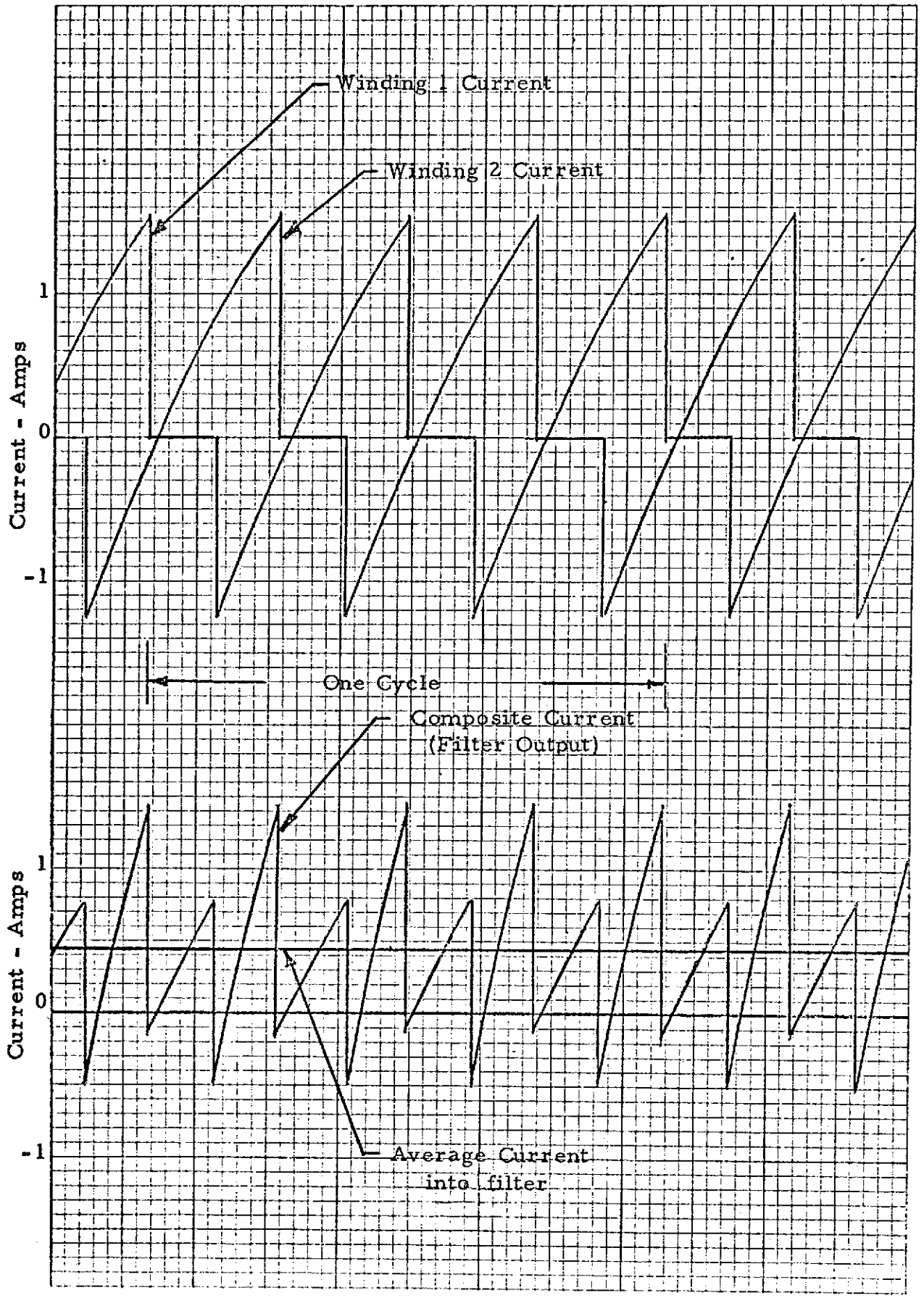

FIGURE 7 SUPPLY CURRENT